

## STABLE MULTIREOLUTION ANALYSIS ON TRIANGLES FOR SURFACE COMPRESSION\*

JAN MAES<sup>†</sup> AND ADHEMAR BULTHEEL<sup>†</sup>

*Dedicated to Ed Saff on the occasion of his 60th birthday*

**Abstract.** Recently we developed multiscale spaces of  $C^1$  piecewise quadratic polynomials on the Powell–Sabin 6-split of a triangulation relative to arbitrary polygonal domains  $\Omega \subset \mathbb{R}^2$ . These multiscale bases are weakly stable with respect to the  $L_2$  norm. In this paper we prove that these multiscale spaces form a multiresolution analysis for the Banach space  $C^1(\overline{\Omega})$  and we show that the multiscale basis forms a strongly stable Riesz basis for the Sobolev spaces  $H^s(\Omega)$  with  $s \in (2, \frac{5}{2})$ . In other words, the norm of a function  $f \in H^s(\Omega)$  can be determined from the size of the coefficients in the multiscale representation of  $f$ . This property makes the multiscale basis suitable for surface compression. A simple algorithm for compression is proposed and we give an optimal a priori error bound that depends on the smoothness of the input surface and on the number of terms in the compressed approximant.

**Key words.** hierarchical bases, Powell–Sabin splines, wavelets, stable approximation by splines, surface compression

**AMS subject classifications.** 41A15, 65D07, 65T60, 41A63

**1. Introduction.** Nowadays surfaces in Computer-Aided Geometric Design are often described with millions of control parameters. These control parameters can for instance arise from measurements of a physical model. Surface compression, which is in fact a trade-off between maintaining accuracy and reduction of the amount of data, is essential in these settings. In [13] a surface compression algorithm was given by means of wavelet decompositions of certain box splines and error bounds were given in terms of the smoothness of the input surface. The purpose of this paper is to extend these ideas to the case of a multiresolution analysis over triangles, based on quadratic Hermite interpolation.

The construction of a multiresolution analysis over a triangulation is closely related to the construction of nested spline spaces. Previous work in this subject has been done on uniform triangulations (see for example [6, 33]). Recently Vanraes *et al.* [31] developed multiscale spaces of  $C^1$  piecewise quadratic polynomials on the Powell–Sabin 6-split of a triangulation relative to arbitrary polygonal domains  $\Omega \subset \mathbb{R}^2$ . The paper [31] is mainly focused on the construction of Powell–Sabin spline wavelets with one vanishing moment. We will concentrate here on the theoretical properties of the corresponding hierarchical basis, and relate this basis to the fairly general definition of multiresolution analysis following the work in [3, 7, 8]. The insights we gain will be used in determining an optimal a priori error bound for surface compression.

DEFINITION 1.1. *A multiresolution analysis consists of*

1. *A Banach space  $\mathcal{B}$  of functions defined on a bounded subset  $\Omega \subset \mathbb{R}^2$  with associated norm  $\|\cdot\|_{\mathcal{B}}$ .*
2. *A nested sequence of subspaces  $S_0 \subset S_1 \subset S_2 \subset \dots \subset \mathcal{B}$  that are dense in  $\mathcal{B}$ ,*

$$\overline{\mathcal{S}} = \mathcal{B} \quad \text{with} \quad \mathcal{S} := \cup_{l \geq 0} S_l.$$

---

\*Received December 2, 2004. Accepted for publication November 30, 2005. Recommended by I. Sloan. This work is partially supported by the Flemish Fund for Scientific Research (FWO Vlaanderen) project MISS (G.0211.02), and by the Belgian Programme on Interuniversity Attraction Poles, initiated by the Belgian Federal Science Policy Office. The scientific responsibility rests with the authors.

<sup>†</sup>Department of Computer Science, Katholieke Universiteit Leuven, Celestijnenlaan 200A, B-3001 Heverlee, Belgium (jan.maes@cs.kuleuven.be).

3. A collection of uniformly bounded operators

$$Q_l : \mathcal{B} \rightarrow S_l$$

with the properties

$$\begin{aligned} Q_l Q_l &= Q_l, \\ Q_l Q_{l+1} &= Q_l, \\ Q_l(\mathcal{B}) &= S_l \end{aligned}$$

for all integers  $l \geq 0$ .

We are interested in how much an approximation  $f_l \in S_l$  of a given function  $f \in \mathcal{B}$  changes when progressing to the next higher resolution  $S_{l+1}$ . Therefore we look for suitable complement spaces  $W_l$  such that

$$S_{l+1} = S_l \oplus W_l$$

as well as for stable bases  $\psi_l := \{\psi_{m,l} : m \in J_l\}$  of  $W_l$  by which one can describe the differences between the approximations  $f_l \in S_l$  and  $f_{l+1} \in S_{l+1}$ . Here  $J_l$  denotes an index set that will be specified more clearly later on. With the projectors  $Q_l$  given, we can define these complement spaces as

$$W_l = \{s \in S_{l+1} | Q_l s = 0\}.$$

Hence we get a decomposition of  $\mathcal{B}$  as the direct sum

$$\mathcal{B} = S_0 \oplus W_0 \oplus W_1 \oplus W_2 \oplus \dots$$

We will refer to the complement spaces  $W_l$  as wavelet spaces and the functions  $\psi_{m,l} \in W_l$  as wavelets, despite the fact that they have no vanishing moment. The spaces  $S_l$  are spanned by bases  $\phi_l = \{\phi_{m,l} : m \in I_l\}$  with  $I_l$  and index set, and we refer to the functions  $\phi_{m,l}$  as scaling functions. Then any  $f_n \in S_n$  can be written in single scale representation

$$(1.1) \quad f_n = \sum_{m \in I_n} c_m \phi_{m,n}$$

or in multiscale representation

$$(1.2) \quad f_n = \sum_{l=-1}^{n-1} \sum_{m \in J_l} d_{m,l} \psi_{m,l},$$

where we have set for simplicity  $\psi_{-1} := \phi_0$ ,  $J_{-1} := I_0$ . Because the spaces  $S_l$  are dense in  $\mathcal{B}$ , every function  $f \in \mathcal{B}$  has a representation (1.2) with  $n \rightarrow \infty$ .

For surface compression purposes the decomposition (1.2) is particularly useful if the norm of  $f$  in some  $L_p$  space or Sobolev space can be determined solely by examining the size of the coefficients  $d_{m,l}$  because we do not want that the overall shape of the surface alters much if we set a small coefficient  $d_{m,l}$  equal to zero. In other words, we want that the multiscale basis forms a strongly stable basis for some  $L_p$  space or Sobolev space.

**DEFINITION 1.2.** Let  $\mathcal{B}$  be a Banach space with a multiresolution analysis and corresponding multiscale basis  $\psi := \bigcup_{l=-1}^{\infty} \psi_l$ . The multiscale basis  $\psi$  is said to form a weakly stable basis for  $\mathcal{B}$  if for each  $n \geq 0$

$$C_{1,n}^{-1} \left\| (d_{m,l})_{l \in K_n, m \in J_l} \right\|_v \leq \left\| \sum_{l \in K_n} \sum_{m \in J_l} d_{m,l} \psi_{m,l} \right\|_{\mathcal{B}} \leq C_{2,n} \left\| (d_{m,l})_{l \in K_n, m \in J_l} \right\|_v,$$

where  $\|\cdot\|_v$  is some yet unspecified vector norm,  $K_n := \{-1, \dots, n-1\}$ , and the constants  $C_{1,n}$  and  $C_{2,n}$  have at most polynomial growth in  $n$ . If the constants  $C_{1,n}$  and  $C_{2,n}$  are independent of  $n$ , the basis is said to be strongly stable.

In Section 2 we recall how to calculate the decomposition (1.2) for the Powell–Sabin spline wavelets, and we discuss their stability with respect to the  $L_2$  norm. In Section 3 we look for a suitable Banach space  $\mathcal{B}$  and operators  $Q_l$  such that the wavelets that span the hierarchical basis form a multiresolution analysis as in Definition 1.1. The stability of the hierarchical basis with respect to the norm in  $\mathcal{B}$  is also investigated and we find that it is a weakly stable basis for  $\mathcal{B}$ . As noted before, an important feature of the decomposition (1.2) for  $f$  is that there exist function spaces such that the multiscale basis is a strongly stable basis with respect to these function spaces. We prove that the hierarchical basis is a strongly stable basis with respect to the Sobolev spaces  $H^s(\Omega)$  with  $s \in (2, \frac{5}{2})$  in Section 4. An algorithm and a priori error bound for surface compression with Powell–Sabin spline wavelets are given in Section 5. Following the framework developed by DeVore *et al.* in [13] we show that the compressed approximant  $S$  of  $f \in B_\sigma^s(L_\sigma(\Omega))$  with at most  $N$  terms satisfies

$$\|f - S\|_{L_\infty(\Omega)} \leq C |f|_{B_\sigma^s(L_\sigma(\Omega))} N^{-s/2}, \quad s < 3.$$

Here  $B_\sigma^s(L_\sigma(\Omega))$  is a Besov space that will be introduced in Section 4.1. We also give sufficient numerical evidence of these error bounds.

We close this introduction with some remarks about notation. The constants that appear in inequalities are denoted by  $C$  and they may vary at each occurrence. Sometimes we use the notation  $A \sim B$  which means that there exist constants  $C_1$  and  $C_2$  such that  $C_1 A \leq B \leq C_2 A$ . Similarly  $A \lesssim B$  expresses that there exists a constant  $C$  such that  $A \leq CB$ .

**2. Powell–Sabin spline wavelets.** In this section we briefly summarize the construction of the Powell–Sabin spline wavelets from [31] and the corresponding hierarchical basis.

Let  $\Omega$  be a domain in  $\mathbb{R}^2$  with polygonal boundary  $\partial\Omega$ . Suppose we have a conforming triangulation  $\Delta$  of  $\Omega$ , constituted of triangles  $T_j$ ,  $j = 1, \dots, t$  and vertices  $V_k$ ,  $k = 1, \dots, N$ . Then  $\Delta^{PS}$  is a Powell–Sabin refinement of  $\Delta$  which divides each triangle  $T_j$  into six smaller triangles with a common vertex  $Z_j$  as indicated on Figure 2.1(a). Now we consider the space

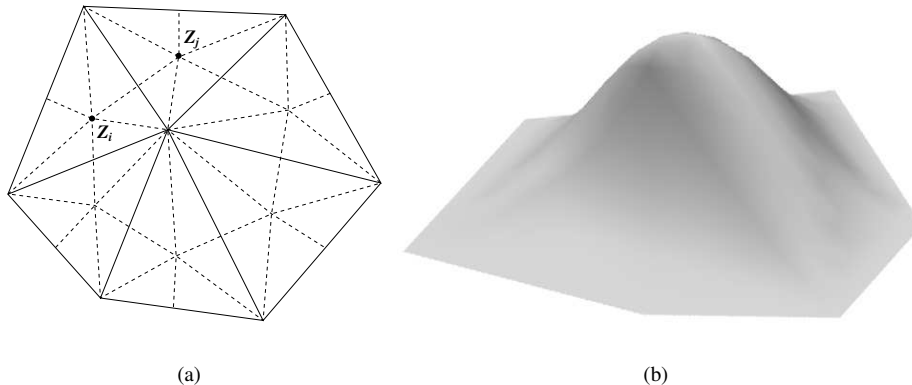


FIG. 2.1. (a) A PS refinement  $\Delta^{PS}$  of  $\Delta$ . The solid lines represent the triangles  $T_j$  of  $\Delta$ . The dotted lines represent the PS refinement. (b) A B-spline basis function.

of  $C^1$  piecewise quadratic polynomials on  $\Delta^{PS}$ , the Powell–Sabin splines,

$$(2.1) \quad S_2^1(\Delta^{PS}) = \{s \in C^1(\Omega) \mid s|_T \in \mathcal{P}_2 \text{ for all } T \in \Delta^{PS}\},$$

where  $\mathcal{P}_2$  is the space of all bivariate polynomials of total degree at most 2. Each of the  $6t$  triangles resulting from the PS-refinement becomes the domain triangle of a quadratic bivariate Bézier polynomial [20, 28, 19]. Powell and Sabin [27] proved that the interpolation problem

$$(2.2) \quad s(V_k) = f(V_k), \quad D_x s(V_k) = D_x f(V_k), \quad D_y s(V_k) = D_y f(V_k), \quad \forall V_k \in \Delta$$

has a unique solution. So, given the function and derivative values at each vertex  $V_k$  of  $\Delta$ , the spline is uniquely defined. Hence the spline space  $S_2^1(\Delta^{PS})$  has dimension  $3N$ .

Dierckx [18] presented a normalized B-spline representation for piecewise polynomials  $s(x, y) \in S_2^1(\Delta^{PS})$

$$(2.3) \quad s(x, y) = \sum_{i=1}^N \sum_{j=1}^3 c_{ij} B_{ij}(x, y), \quad (x, y) \in \Omega$$

where the basis functions form a convex partition of unity

$$(2.4) \quad B_{ij}(x, y) \geq 0,$$

$$(2.5) \quad \sum_{i=1}^N \sum_{j=1}^3 B_{ij}(x, y) = 1,$$

and have local support:  $B_{ij}$  vanishes outside the union of all triangles  $T \in \Delta$  containing  $V_i$ . One such basis function is depicted in Figure 2.1(b). Each basis function  $B_{ij}$  is the unique solution of the interpolation problem (2.2) with

$$(2.6) \quad B_{ij}(V_k) = \delta_{ik} \alpha_{ij}, \quad D_x B_{ij}(V_k) = \delta_{ik} \beta_{ij}, \quad D_y B_{ij}(V_k) = \delta_{ik} \gamma_{ij}, \quad \forall V_k \in \Delta$$

where  $\delta_{ij}$  is the Kronecker delta and  $(\alpha_{ij}, \beta_{ij}, \gamma_{ij})$ ,  $j = 1, 2, 3$  are three linearly independent triplets of real numbers. The values of these real numbers are determined from the algorithm described in [18].

In [32], Vanraes *et al.* present a subdivision scheme to compute a representation (2.3) of a PS-spline on a triadic refinement  $\Delta_{l+1}$  of  $\Delta_l$ . The subscript  $l$  denotes the resolution level. This subdivision scheme is used as the prediction step in the Lifting Scheme [30] to create second generation Powell–Sabin spline wavelets. Figure 2.2 explains the principle of triadic refinement. We place two new vertices on every edge of the current triangulation, each at one side of the intersection with the PS-refinement, and one new vertex is placed on the position of every interior point  $Z_j$  in the PS-refinement. Throughout the paper we assume that some initial triangulation  $\Delta_0$  is given and that the triadic refinement procedure yields nested sequences

$$(2.7) \quad \Delta_0 \subset \Delta_1 \subset \Delta_2 \subset \dots$$

$$(2.8) \quad \Delta_0^{PS} \subset \Delta_1^{PS} \subset \Delta_2^{PS} \subset \dots$$

that are “regular”, which means that the minimum angle of any triangle in any  $\Delta_l$  remains bounded away from zero and that

$$(2.9) \quad 3^{-l} \lesssim \min_{T \in \Delta_l} |T| \leq \max_{T \in \Delta_l} |T| \lesssim 3^{-l}, \quad l \in \mathbb{N}_0,$$

where  $|T|$  is the diameter of triangle  $T$ . The same is valid for the triangles in the PS-refinement

$$3^{-l} \lesssim \min_{T \in \Delta_l^{PS}} |T| \leq \max_{T \in \Delta_l^{PS}} |T| \lesssim 3^{-l}, \quad l \in \mathbb{N}_0.$$

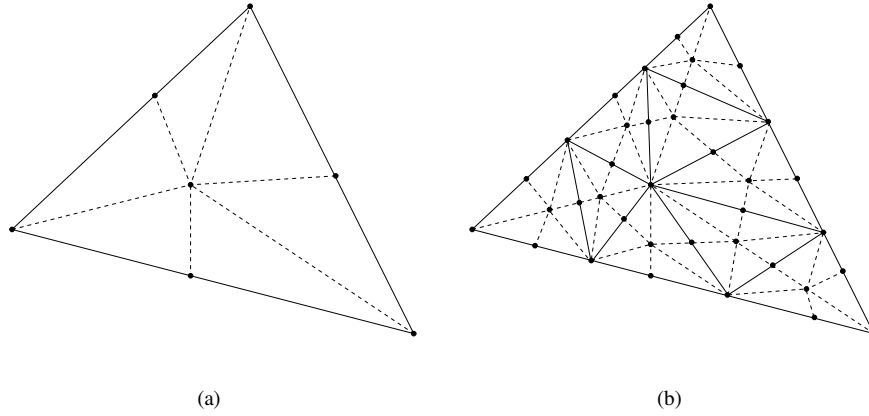


FIG. 2.2. Principle of triadic refinement. We place a new vertex at the position of the interior point in the PS-refinement and two new vertices on each edge, one at each side of the intersection with the PS-refinement.

With each triangulation  $\Delta_l$  we have a corresponding B-spline basis  $\{B_{ij,l}\}_{i=1,j=1,2,3}^{N_l}$  for the space  $S_l := S_2^1(\Delta_l^{PS})$ .

From (2.3) and (2.6) we have

$$\begin{bmatrix} s_l(V_i) \\ D_x s_l(V_i) \\ D_y s_l(V_i) \end{bmatrix} = \mathbf{A}_{i,l} \begin{bmatrix} c_{i1} \\ c_{i2} \\ c_{i3} \end{bmatrix} \quad \text{with} \quad \mathbf{A}_{i,l} = \begin{bmatrix} \alpha_{i1,l} & \alpha_{i2,l} & \alpha_{i3,l} \\ \beta_{i1,l} & \beta_{i2,l} & \beta_{i3,l} \\ \gamma_{i1,l} & \gamma_{i2,l} & \gamma_{i3,l} \end{bmatrix}, \quad i = 1, \dots, N_l.$$

This gives rise to quasi-interpolant operators  $Q_l : C^1(\bar{\Omega}) \rightarrow S_l$  given by

$$(2.10) \quad Q_l f(x, y) = \sum_{i=1}^{N_l} \sum_{j=1}^3 \mu_{ij,l}(f) B_{ij,l}(x, y),$$

where the  $\mu_{ij,l}$  are linear functionals of the form

$$\begin{bmatrix} \mu_{i1,l}(f) \\ \mu_{i2,l}(f) \\ \mu_{i3,l}(f) \end{bmatrix} := (\mathbf{A}_{i,l})^{-1} \begin{bmatrix} f(V_i) \\ D_x f(V_i) \\ D_y f(V_i) \end{bmatrix}.$$

It is proved in [23] that these linear functionals can be rewritten as

$$(2.11) \quad \mu_{ij,l}(f) = f(V_i) + \eta_{ij,l} D_x f(V_i) + \tilde{\eta}_{ij,l} D_y f(V_i)$$

where the  $\eta_{ij,l}$  and  $\tilde{\eta}_{ij,l}$  satisfy

$$(2.12) \quad |\eta_{ij,l}| \lesssim 3^{-l}, \quad |\tilde{\eta}_{ij,l}| \lesssim 3^{-l}.$$

Note that this quasi-interpolant  $Q_l f$  is in fact the Hermite interpolant of  $f$  in the space  $S_l$ . This Hermite interpolant can also be expressed [28] e.g. in the Hermite basis as follows. Setting  $e_1$  and  $e_2$  as the unit directions corresponding to the coordinate axes, we have

$$Q_l f = \sum_{i=1}^{N_l} (f(V_i) \phi_i + \nabla f(V_i) e_1 \chi_i + \nabla f(V_i) e_2 \psi_i)$$

where  $\phi_i(V_j) = \nabla\chi_i(V_j)e_1 = \nabla\psi_i(V_j)e_2 = \delta_{ij}$ , the other Hermite data being zero. See also [25] for other kinds of PS quasi-interpolants.

Clearly the operator  $Q_l$  satisfies

$$Q_l s_l = s_l, \quad \forall s_l \in S_l,$$

and

$$Q_l f(V_i) = f(V_i), \quad \nabla Q_l f(V_i) = \nabla f(V_i), \quad i = 1, \dots, N_l.$$

From the work in [24] we know that the B-spline functions form a stable basis for the  $L_\infty$  norm, i.e.,

$$(2.13) \quad \left\| \sum_{i=1}^{N_l} \sum_{j=1}^3 c_{ij} B_{ij,l}(x, y) \right\|_{L_\infty(\Omega)} \sim \|c\|_\infty.$$

In [31] it is proved that the B-spline functions (under a suitable normalization) are stable with respect to the  $L_p$  norm for all values  $p \geq 1$ . We give a new proof here which extends the range of stability to all  $p > 0$ . Note that  $\|\cdot\|_{L_p}$  is not really a norm but a semi-norm if  $p < 1$ .

**THEOREM 2.1.** *If  $s_l = \sum_{i=1}^{N_l} \sum_{j=1}^3 \mu_{ij,l}(s_l) B_{ij,l}$  is in  $S_l$ , then for any  $0 < p \leq \infty$  we have*

$$(2.14) \quad \|s_l\|_{L_p(\Omega)} \sim \left( \sum_{i=1}^{N_l} \sum_{j=1}^3 |\mu_{ij,l}(s_l)|^p 3^{-2l} \right)^{1/p}$$

*Proof.* Using the Markov inequality for polynomials (see e.g. [4, 22]), (2.11) and (2.12) we infer that

$$|\mu_{ij,l}(s_l)| \lesssim \|s_l\|_{L_\infty(T_i)}$$

with  $T_i \in \Delta_l^{PS}$  such that  $V_i \in T_i$ . By mapping  $T_i$  to the standard simplex  $T_s := \{(x, y) \mid 0 \leq x, y \leq 1, x + y \leq 1\}$ , and using the fact that all norms on the finite dimensional space of polynomials are equivalent, it is easy to see that

$$\|s_l\|_{L_\infty(T_i)} \lesssim 3^{2l/p} \|s_l\|_{L_p(T_i)}$$

which implies

$$\left( \sum_{i=1}^{N_l} \sum_{j=1}^3 |\mu_{ij,l}(s_l)|^p 3^{-2l} \right)^{1/p} \lesssim \left( \sum_{i=1}^{N_l} \sum_{j=1}^3 \|s_l\|_{L_p(T_i)}^p \right)^{1/p} \lesssim \|s_l\|_{L_p(\Omega)}.$$

The other inequality follows from the observation that

$$\left| \sum_{i=1}^{N_l} \sum_{j=1}^3 \mu_{ij,l}(s_l) B_{ij,l}(x, y) \right|^p \lesssim \sum_{i=1}^{N_l} \sum_{j=1}^3 |\mu_{ij,l}(s_l)|^p |B_{ij,l}(x, y)|^p,$$

which holds because at any  $(x, y) \in \Omega$  there are at most 9 nonzero B-splines. We find that

$$\begin{aligned}
 \|s_l\|_{L^p(\Omega)}^p &= \int_{\Omega} \left| \sum_{i=1}^{N_l} \sum_{j=1}^3 \mu_{ij,l}(s_l) B_{ij,l}(x, y) \right|^p dx dy \\
 &\lesssim \sum_{i=1}^{N_l} \sum_{j=1}^3 |\mu_{ij,l}(s_l)|^p \int_{\Omega} |B_{ij,l}(x, y)|^p dx dy \\
 &\lesssim \sum_{i=1}^{N_l} \sum_{j=1}^3 |\mu_{ij,l}(s_l)|^p 3^{-2l}. \quad \square
 \end{aligned}$$

It is convenient to write the following in matrix form. Because  $L_2$  stability is important for wavelets we define the scaling functions  $\phi_l$  as  $3^l \mathbf{B}_l$  with  $\mathbf{B}_l$  the row vector of basis functions  $B_{ij,l}$  such that

$$s_l(x, y) = \phi_l \mathbf{c}_l \quad \text{and} \quad \|\phi_l \mathbf{c}_l\|_{L_2(\Omega)} \sim \|\mathbf{c}_l\|_{l_2}.$$

Similarly we define  $\psi_l$  as a set of basis functions for  $W_l$ . A spline  $s_{l+1}$  in  $S_{l+1} = S_l \oplus W_l$  can now be written as

$$s_{l+1}(x, y) = \phi_l \mathbf{c}_l + \psi_l \mathbf{d}_l.$$

From the construction in [31] we know that there exist matrices  $\mathbf{P}_l$  and  $\mathbf{Q}_l$  such that

$$(2.15) \quad [\phi_l \quad \psi_l] = \phi_{l+1} [\mathbf{P}_l \quad \mathbf{Q}_l],$$

and such that the wavelets  $\psi_l$  (see Figure 2.3a) have one vanishing moment, i.e. they satisfy

$$\langle 1, \psi_{m,l} \rangle_{L_2(\Omega)} = 0, \quad \forall \psi_{m,l} \in \psi_l.$$

However, in this paper we take  $\mathbf{Q}_l$  equal to the identity matrix  $\mathbf{I}$ , which yields a so-called hierarchical basis, and the wavelets  $\psi_{m,l}$  lose their vanishing moment (see Figure 2.3b). In fact the wavelets are scaling functions at a higher resolution level.

Denote  $\mathbf{M}_l = [\mathbf{P}_l \quad \mathbf{Q}_l]$ . The following results are valid for both the wavelet basis with vanishing moment and the hierarchical basis. We can find a multiscale representation for  $\phi_{l+1}$  as

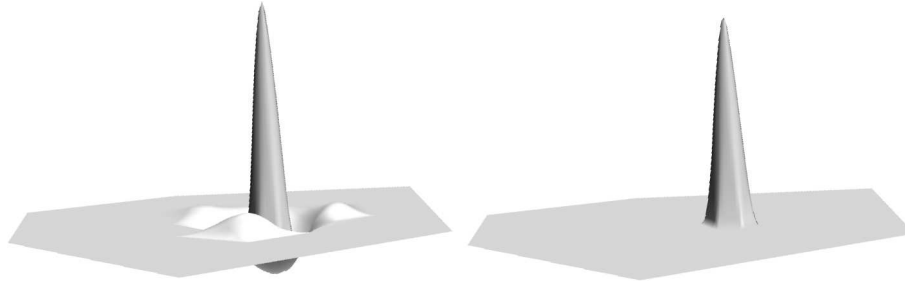
$$[\phi_0 \quad \psi_0 \quad \psi_1 \cdots \psi_{l-1} \quad \psi_l] = \phi_{l+1} \mathbf{T}_l,$$

$$\mathbf{T}_l = \begin{bmatrix} \mathbf{M}_l & \mathbf{0} \\ \mathbf{0} & \mathbf{I} \end{bmatrix} \begin{bmatrix} \mathbf{M}_{l-1} & \mathbf{0} \\ \mathbf{0} & \mathbf{I} \end{bmatrix} \cdots \begin{bmatrix} \mathbf{M}_0 & \mathbf{0} \\ \mathbf{0} & \mathbf{I} \end{bmatrix}.$$

By computing the wavelet transform there should be no significant loss of accuracy in the data, or in other words the condition numbers should remain uniformly bounded

$$(2.16) \quad \|\mathbf{T}_l\|_2, \|(\mathbf{T}_l)^{-1}\|_2 = \mathcal{O}(1), \quad l \rightarrow \infty.$$

From Dahmen [7, 8] we know that the wavelet transform  $\mathbf{T}_l$  is uniformly stable, i.e. (2.16) holds, if the multiscale basis  $\psi := \bigcup_{l=-1}^{\infty} \psi_l$  is a Riesz basis, where we set for simplicity  $\psi_{-1} := \phi_0$ . A necessary condition is that each basis  $\psi_l$  is a uniformly stable Riesz basis



(a) The Powell–Sabin wavelet from [31].

(b) The corresponding wavelet from the hierarchical basis, i.e. with  $\mathbf{Q}_l \equiv \mathbf{I}$ .

FIG. 2.3. Two constructions of Powell–Sabin spline wavelets  $\psi_{m,l}$ . In this paper we will be working with the hierarchical basis.

or alternatively that the condition numbers of the one level transforms  $\mathbf{M}_l$  are uniformly bounded in  $l$ , i.e.

$$(2.17) \quad \|\mathbf{M}_l\|_2, \|(\mathbf{M}_l)^{-1}\|_2 = \mathcal{O}(1).$$

From the work in [31] we know that

$$(2.18) \quad \|\mathbf{M}_l\|_\infty, \|(\mathbf{M}_l)^{-1}\|_\infty = \mathcal{O}(1),$$

$$(2.19) \quad \|\mathbf{M}_l\|_1, \|(\mathbf{M}_l)^{-1}\|_1 = \mathcal{O}(1).$$

This yields (2.17) because  $\|\cdot\|_2^2 \leq \|\cdot\|_\infty \|\cdot\|_1$  and the wavelets  $\psi_l$  form a  $L_2$ -stable Riesz basis for  $W_l$ . Evidently the basis  $\phi_l \cup \psi_l$  is also a  $L_2$ -stable Riesz basis for  $S_{l+1}$  and the multiscale basis  $\psi$  forms a weakly stable basis for  $L_2(\Omega)$ . For references to wavelets, see also the surveys [5], [9] and [10].

Note that in the rest of the paper we shall work with the hierarchical basis, i.e. take  $\mathbf{Q}_l$  equal to the identity matrix  $\mathbf{I}$  in (2.15).

**3. Multiresolution analysis.** In the previous section we constructed a nested sequence of subspaces  $S_0 \subset S_1 \subset S_2 \subset \dots$  and we introduced an operator  $Q_l$ . In this section we look for a Banach space  $\mathcal{B}$  such that sequence of subspaces  $\{S_l\}_{l=0}^\infty$  and the operators  $Q_l$  form a multiresolution analysis in the sense of Definition 1.1. Furthermore we will investigate the stability of the multiscale basis  $\psi$  with respect to  $\mathcal{B}$ .

**3.1. A Banach space with suitable operators.** As Banach space  $\mathcal{B}$  we take  $C^1(\overline{\Omega})$ , the space of functions defined on  $\overline{\Omega}$  that are continuous and have continuous first derivatives in  $\overline{\Omega}$ . There is a natural norm for  $C^1(\overline{\Omega})$  which is defined as

$$(3.1) \quad \|f\|_{C^1(\overline{\Omega})} := \max \left\{ \|f\|_{L_\infty(\Omega)}, \|D_x f\|_{L_\infty(\Omega)}, \|D_y f\|_{L_\infty(\Omega)} \right\}$$

and every function  $f$  in  $C^1(\overline{\Omega})$  satisfies  $\|f\|_{C^1(\overline{\Omega})} < \infty$ .

The following proposition shows that the operators  $Q_l$  from (2.10) are suitable for constructing a multiresolution analysis.

PROPOSITION 3.1. *For each  $l \geq 0$  we have*

$$Q_l Q_{l+1} = Q_l.$$

*Proof.* From the construction of  $Q_l$  we know that

$$Q_{l+1} f(V_k) = f(V_k), \quad \nabla Q_{l+1} f(V_k) = \nabla f(V_k), \quad \forall V_k \in \Delta_{l+1}.$$

Then it is also obvious that

$$Q_l Q_{l+1} f(V_k) = f(V_k), \quad \nabla Q_l Q_{l+1} f(V_k) = \nabla f(V_k), \quad \forall V_k \in \Delta_l \subset \Delta_{l+1},$$

and

$$Q_l f(V_k) = f(V_k), \quad \nabla Q_l f(V_k) = \nabla f(V_k), \quad \forall V_k \in \Delta_l \subset \Delta_{l+1}.$$

From the uniqueness of the interpolation problem (2.2) we conclude that  $Q_l Q_{l+1} = Q_l$ .  $\square$

There are still two properties required for a multiresolution analysis that we did not prove, namely that the space  $\mathcal{S}$  is dense in  $C^1(\bar{\Omega})$  and that the projectors  $Q_l$  are uniformly bounded.

PROPOSITION 3.2. *For every  $f \in C^1(\bar{\Omega})$  and every point  $(x, y) \in \bar{\Omega}$  the inequalities*

$$(3.2) \quad |Q_l f(x, y)| \lesssim \|f\|_{C^1(\bar{\Omega})},$$

$$(3.3) \quad |D_x Q_l f(x, y)| \lesssim \|f\|_{C^1(\bar{\Omega})},$$

$$(3.4) \quad |D_y Q_l f(x, y)| \lesssim \|f\|_{C^1(\bar{\Omega})}$$

*hold. Therefore the operators  $Q_l$  are uniformly bounded in  $C^1(\bar{\Omega})$ .*

*Proof.* The inequalities

$$(3.5) \quad |Q_l f(x, y)| \leq \max_{i,j} |\mu_{ij,l}(f)| \left| \sum_{i=1}^{N_l} \sum_{j=1}^3 B_{ij,l}(x, y) \right| \lesssim \|f\|_{C^1(\bar{\Omega})}$$

hold because of (2.5), (2.11) and (2.12). The other two inequalities (3.3) and (3.4) are similar, so we only give proof of the first one. We have

$$\begin{aligned} |D_x Q_l f(x, y)| &= \left| \sum_{i=1}^{N_l} \sum_{j=1}^3 \mu_{ij,l}(f) D_x B_{ij,l}(x, y) \right| \\ &\lesssim \left| \sum_{i=1}^{N_l} \sum_{j=1}^3 f(V_i) D_x B_{ij,l}(x, y) \right| + \left| \sum_{i=1}^{N_l} \sum_{j=1}^3 3^{-l} \|f\|_{C^1(\bar{\Omega})} D_x B_{ij,l}(x, y) \right|. \end{aligned}$$

Now suppose that  $(x, y)$  belongs to triangle  $T \in \Delta_l$  with vertices  $V_1, V_2$  and  $V_3$ . Then we deduce from the local support of the basis functions that

$$(3.6) \quad |D_x Q_l f(x, y)| \lesssim \left| \sum_{i=1}^3 \sum_{j=1}^3 f(V_i) D_x B_{ij,l}(x, y) \right| + \left| \sum_{i=1}^3 \sum_{j=1}^3 3^{-l} \|f\|_{C^1(\overline{\Omega})} D_x B_{ij,l}(x, y) \right|.$$

From the Markov inequality for polynomials in  $\mathcal{P}_2$  (see e.g. [22]), the regularity (2.9), and Equation (2.13) it follows that

$$(3.7) \quad |D_x B_{ij,l}(x, y)| \lesssim 3^l.$$

Hence the second part of (3.6) can be bounded by  $C_2 \|f\|_{C^1(\overline{\Omega})}$  with  $C_2$  a constant. To prove that the first part is bounded by  $C_1 \|f\|_{C^1(\overline{\Omega})}$  we need the following simple property that

$$(3.8) \quad \sum_{i=1}^3 \sum_{j=1}^3 D_x B_{ij,l}(x, y) = 0,$$

which follows immediately from (2.5). Using (3.8) and the mean-value theorem the first part of (3.6) can be bounded by

$$\begin{aligned} \left| \sum_{i=1}^3 \sum_{j=1}^3 f(V_i) D_x B_{ij,l}(x, y) \right| &= \left| \sum_{j=1}^3 (f(V_2) - f(V_1)) D_x B_{2j,l}(x, y) \right. \\ &\quad \left. + (f(V_3) - f(V_1)) D_x B_{3j,l}(x, y) \right| \\ &\lesssim \left| \sum_{j=1}^3 D_{\beta^1} f(\xi^1) 3^{-l} D_x B_{2j,l}(x, y) \right. \\ &\quad \left. + D_{\beta^2} f(\xi^2) 3^{-l} D_x B_{3j,l}(x, y) \right|, \end{aligned}$$

where  $\xi^1$  and  $\xi^2$  are points on the line segments  $[V_1, V_2]$  resp.  $[V_1, V_3]$ , and  $\beta^1$  and  $\beta^2$  are unit directions that point from  $V_1$  to  $V_2$  resp.  $V_3$ . From the Markov inequality (3.7) we deduce that  $|D_x Q_l f(x, y)| \lesssim \|f\|_{C^1(\overline{\Omega})}$ .  $\square$

The following proposition is the last step in showing that the spaces  $\{S_l\}_{l=0}^\infty$  form a multiresolution analysis. We verify that every function in  $C^1(\overline{\Omega})$  can be approximated by functions from  $\mathcal{S}$  with arbitrarily small error.

**PROPOSITION 3.3.** *The space  $\mathcal{S}$  is dense in the Banach space  $C^1(\overline{\Omega})$  with norm  $\|\cdot\|_{C^1(\overline{\Omega})}$ .*

*Proof.* It is sufficient to show that  $\lim_{l \rightarrow \infty} \|f - Q_l f\|_{C^1(\overline{\Omega})} = 0$  for every function  $f \in C^1(\overline{\Omega})$ . As in the proof of Proposition 3.2 let  $(x, y)$  be an arbitrary point in triangle  $T \in \Delta_l$  with vertices  $V_1, V_2$  and  $V_3$ . Then from (2.5), (2.11), (2.12) and the mean-value

theorem we find

$$\begin{aligned}
 |f(x, y) - Q_l f(x, y)| &= \left| f(x, y) \sum_{i=1}^3 \sum_{j=1}^3 B_{ij,l}(x, y) - \sum_{i=1}^3 \sum_{j=1}^3 \mu_{ij,l}(f) B_{ij,l}(x, y) \right| \\
 &\lesssim \left| \sum_{i=1}^3 \sum_{j=1}^3 (f(x, y) - f(V_i)) B_{ij,l}(x, y) \right| \\
 (3.9) \quad &+ \left| \sum_{i=1}^3 \sum_{j=1}^3 \|f\|_{C^1(\bar{\Omega})} 3^{-l} B_{ij,l}(x, y) \right| \\
 &\lesssim \left| \sum_{i=1}^3 \sum_{j=1}^3 D_{\beta^i} f(\xi^i) 3^{-l} B_{ij,l}(x, y) \right| + \|f\|_{C^1(\bar{\Omega})} 3^{-l} \\
 &\lesssim \|f\|_{C^1(\bar{\Omega})} 3^{-l},
 \end{aligned}$$

and we obtain that  $\lim_{l \rightarrow \infty} \|f - Q_l f\|_{L^\infty(\Omega)} = 0$ . Now we prove that the derivatives of  $Q_l f$  converge to the derivatives of  $f$ . We only give the proof for the derivative with respect to  $x$ . Denote the Cartesian coordinates of vertex  $V_k \in \Delta_l$  with  $(x_k, y_k)$ . Then the equations

$$\begin{aligned}
 x &= \sum_{i=1}^{N_l} \sum_{j=1}^3 (x_i + \eta_{ij,l}) B_{ij,l}(x, y), \\
 y &= \sum_{i=1}^{N_l} \sum_{j=1}^3 (y_i + \tilde{\eta}_{ij,l}) B_{ij,l}(x, y)
 \end{aligned}$$

hold. If we take the derivative with respect to  $x$  and we evaluate in  $(x, y) \in T$  then we infer that

$$(3.10) \quad 1 = \sum_{i=1}^3 \sum_{j=1}^3 (x_i + \eta_{ij,l}) D_x B_{ij,l}(x, y),$$

$$(3.11) \quad 0 = \sum_{i=1}^3 \sum_{j=1}^3 (y_i + \tilde{\eta}_{ij,l}) D_x B_{ij,l}(x, y).$$

If we use (3.10) and (3.11) we can deduce that

$$\begin{aligned}
 e &= |D_x f(x, y) - D_x Q_l f(x, y)| \\
 &= \left| D_x f(x, y) \left( \sum_{i=1}^3 \sum_{j=1}^3 (x_i + \eta_{ij,l}) D_x B_{ij,l}(x, y) \right) \right. \\
 &\quad \left. + D_y f(x, y) \left( \sum_{i=1}^3 \sum_{j=1}^3 (y_i + \tilde{\eta}_{ij,l}) D_x B_{ij,l}(x, y) \right) \right. \\
 &\quad \left. - \sum_{i=1}^3 \sum_{j=1}^3 (f(V_i) + \eta_{ij,l} D_x f(V_i) + \tilde{\eta}_{ij,l} D_y f(V_i)) D_x B_{ij,l}(x, y) \right|.
 \end{aligned}$$

If we use (3.8) we can rewrite  $e$  as

$$\begin{aligned}
 e = & \left| \sum_{i=1}^3 \sum_{j=1}^3 (D_x f(x, y) - D_x f(V_i)) \eta_{ij,l} D_x B_{ij,l}(x, y) \right. \\
 & + \sum_{i=1}^3 \sum_{j=1}^3 (D_y f(x, y) - D_y f(V_i)) \tilde{\eta}_{ij,l} D_x B_{ij,l}(x, y) \\
 & + D_x f(x, y) \sum_{j=1}^3 ((x_2 - x_1) D_x B_{2j,l}(x, y) + (x_3 - x_1) D_x B_{3j,l}(x, y)) \\
 & + D_y f(x, y) \sum_{j=1}^3 ((y_2 - y_1) D_x B_{2j,l}(x, y) + (y_3 - y_1) D_x B_{3j,l}(x, y)) \\
 & \left. - \sum_{j=1}^3 ((f(V_2) - f(V_1)) D_x B_{2j,l}(x, y) + (f(V_3) - f(V_1)) D_x B_{3j,l}(x, y)) \right|
 \end{aligned}$$

and from (2.12), (3.7) and the mean-value theorem we get

$$\begin{aligned}
 (3.12) \quad e \leq & \left| \sum_{i=1}^3 \sum_{j=1}^3 C_1 (D_x f(x, y) - D_x f(V_i)) \right| \\
 & + \left| \sum_{i=1}^3 \sum_{j=1}^3 C_2 (D_y f(x, y) - D_y f(V_i)) \right| \\
 & + \left| \sum_{j=1}^3 \langle \nabla f(x, y) - \nabla f(\xi^1), V_2 - V_1 \rangle D_x B_{2j}(x, y) \right. \\
 & \left. + \langle \nabla f(x, y) - \nabla f(\xi^2), V_3 - V_1 \rangle D_x B_{3j}(x, y) \right|,
 \end{aligned}$$

where  $\xi^1$  and  $\xi^2$  are points on the line segments  $[V_1, V_2]$  resp.  $[V_1, V_3]$ , and  $\langle \cdot, \cdot \rangle$  is the usual dot product. The upper bound in (3.12) goes to 0 as  $l \rightarrow \infty$  because of the uniform continuity of the partial derivatives of  $f$ .  $\square$

REMARK 3.4. Note that Propositions 3.2 and 3.3 are inherent to the spline spaces  $S_l$  and do not depend on any particular basis. Therefore one can prove these propositions using any basis for  $S_l$  that is stable in the sense of (2.13), such as for instance the Hermite basis of [28].

**3.2. Stability in the Banach space.** From (2.17) we know that the multiscale basis  $\psi$  forms a weakly stable basis for  $L_2(\Omega)$ . In this subsection we prove that under a suitable normalization the multiscale basis forms a weakly stable basis for  $C^1(\overline{\Omega})$ . Define the normalized scaling functions  $\zeta_{ij,l}$  as

$$(3.13) \quad \zeta_{ij,l}(x, y) := 3^{-l} B_{ij,l}(x, y)$$

and define the normalized wavelet functions  $\xi_{m,l}$  as

$$(3.14) \quad \xi_{m,l}(x, y) := 3^{-2l} \psi_{m,l}(x, y), \quad m \in J_l$$

where  $\psi_{m,l}$  are the Powell–Sabin spline wavelets from Section 2 with  $\mathbf{Q}_l = \mathbf{I}_l$  in (2.15). We need the following lemma.

LEMMA 3.5. *Let  $g_l$  be the wavelet component of  $f$  in  $W_l$  given by*

$$g_l = Q_{l+1}f - Q_l f = \sum_{i=1}^{N_{l+1}} \sum_{j=1}^3 b_{ij,l+1} \zeta_{ij,l+1} = \sum_{m \in J_l} d_{m,l} \xi_{m,l},$$

with  $f$  in  $C^1(\overline{\Omega})$ . Then the coefficients  $b_{ij,l+1}$  and  $d_{m,l}$  are bounded by

$$|b_{ij,l+1}| \lesssim \|g_l\|_{C^1(\overline{\Omega})} \lesssim \|f\|_{C^1(\overline{\Omega})}.$$

$$|d_{m,l}| \lesssim \|g_l\|_{C^1(\overline{\Omega})} \lesssim \|f\|_{C^1(\overline{\Omega})}.$$

Furthermore we have that the estimates

$$\|g_l\|_{L_\infty(\Omega)} \lesssim \|\mathbf{b}_{l+1}\|_\infty, \quad \|g_l\|_{L_\infty(\Omega)} \lesssim \|\mathbf{d}_l\|_\infty,$$

$$\|D_x g_l\|_{L_\infty(\Omega)} \lesssim \|\mathbf{b}_{l+1}\|_\infty, \quad \|D_x g_l\|_{L_\infty(\Omega)} \lesssim \|\mathbf{d}_l\|_\infty,$$

$$\|D_y g_l\|_{L_\infty(\Omega)} \lesssim \|\mathbf{b}_{l+1}\|_\infty, \quad \|D_y g_l\|_{L_\infty(\Omega)} \lesssim \|\mathbf{d}_l\|_\infty$$

hold where  $\|\mathbf{b}_{l+1}\|_\infty := \max_{i,j} \{|b_{ij,l+1}|\}$  and  $\|\mathbf{d}_l\|_\infty := \max_m \{|d_{m,l}|\}$ .

*Proof.* Because  $g_l$  satisfies  $Q_l g_l = 0$  we know that

$$g_l(V_k) = \nabla g_l(V_k) = 0 \quad \text{for all } V_k \in \Delta_l.$$

Because  $g_l \in W_l \subset S_{l+1}$  we have  $Q_{l+1}g_l = g_l$  which yields  $b_{ij,l+1} = 3^{l+1} \mu_{ij,l+1}(g_l)$  and we find that

$$(3.15) \quad b_{ij,l+1} = 0 \quad \text{for all } \{i \mid V_i \in \Delta_l\}.$$

Choose  $i$  such that  $V_i \in \Delta_{l+1} \setminus \Delta_l$ . Let  $k$  be such that  $V_k \in \Delta_l$  and such that  $V_i$  and  $V_k$  are contained in the same triangle  $T \in \Delta_l$ . Then

$$\begin{aligned} |b_{ij,l+1}| &= 3^{l+1} |g_l(V_i) + \eta_{ij,l+1} D_x g_l(V_i) + \tilde{\eta}_{ij,l+1} D_y g_l(V_i)| \\ &\leq 3^{l+1} |g_l(V_i) - g_l(V_k)| + C \|g_l\|_{C^1(\overline{\Omega})} \\ &\lesssim \|g_l\|_{C^1(\overline{\Omega})}, \end{aligned}$$

where the last step follows from the mean-value theorem. Because the operator  $Q_l$  is bounded in  $C^1(\overline{\Omega})$  (Proposition 3.2) we find that  $|b_{ij,l+1}| \lesssim \|f\|_{C^1(\overline{\Omega})}$ .

From (2.13) we immediately find that

$$\|g_l\|_{L_\infty(\Omega)} \lesssim 3^{-(l+1)} \|\mathbf{b}_{l+1}\|_\infty \leq \|\mathbf{b}_{l+1}\|_\infty.$$

Let  $(x, y)$  be an arbitrary point in triangle  $T \in \Delta_{l+1}$  with vertices  $V_1, V_2$  and  $V_3$ . Then the

inequalities

$$\begin{aligned}
 |D_x g_l(x, y)| &= \left| \sum_{i=1}^3 \sum_{j=1}^3 b_{ij,l+1} D_x \zeta_{ij,l+1}(x, y) \right| \\
 &\leq \|\mathbf{b}_{l+1}\|_\infty \sum_{i=1}^3 \sum_{j=1}^3 |D_x \zeta_{ij,l+1}(x, y)| \\
 &\lesssim \|\mathbf{b}_{l+1}\|_\infty \sum_{i=1}^3 \sum_{j=1}^3 3^{l+1} \|\zeta_{ij,l+1}(x, y)\|_{L_\infty(T)} \\
 &\lesssim \|\mathbf{b}_{l+1}\|_\infty
 \end{aligned}$$

hold. We have used the Markov inequality (3.7) and (2.13). This yields

$$\|D_x g_l\|_{L_\infty(\Omega)} \lesssim \|\mathbf{b}_{l+1}\|_\infty$$

and the proof for  $\|D_y g_l\|_{L_\infty(\Omega)}$  is similar.

From (3.15) and the fact that the multiscale basis is a hierarchical basis, we easily infer that

$$\|\mathbf{b}_{l+1}\|_\infty = \|\mathbf{d}_l\|_\infty. \quad \square$$

Most of the work for proving stability in  $C^1(\overline{\Omega})$  is done in Lemma 3.5. We conclude this section with the following theorem.

**THEOREM 3.6.** *Let  $f$  be a function in  $C^1(\overline{\Omega})$  and define the wavelet components  $g_l \in W_l$  as*

$$g_l = Q_{l+1}f - Q_l f = \sum_{m \in J_l} d_{m,l} \xi_{m,l},$$

with the wavelet functions  $\xi_{m,l}$  defined as in (3.14). Then the multiscale wavelet basis is a weakly stable basis for  $C^1(\overline{\Omega})$ , i.e.

$$(3.16) \quad C_1^{-1} \max_{l \leq p-1} \|\mathbf{d}_l\|_\infty \leq \|Q_p f - Q_0 f\|_{C^1(\overline{\Omega})} \leq p C_2 \max_{l \leq p-1} \|\mathbf{d}_l\|_\infty.$$

*Proof.* Suppose  $\max_{l \leq p-1} \|\mathbf{d}_l\|_\infty = \|\mathbf{d}_r\|_\infty$ . Then from Lemma 3.5 we find

$$\begin{aligned}
 \max_{l \leq p-1} \|\mathbf{d}_l\|_\infty &\lesssim \|Q_{r+1}f - Q_r f\|_{C^1(\overline{\Omega})} \\
 &\lesssim \|Q_{r+1}f - Q_0 f\|_{C^1(\overline{\Omega})} + \|Q_r f - Q_0 f\|_{C^1(\overline{\Omega})}
 \end{aligned}$$

Because  $Q_{r+1}Q_p f = Q_{r+1}f$  and  $Q_{r+1}Q_0 f = Q_0 f$  we deduce that

$$\begin{aligned}
 \max_{l \leq p-1} \|\mathbf{d}_l\|_\infty &\lesssim \|Q_{r+1}Q_p f - Q_{r+1}Q_0 f\|_{C^1(\overline{\Omega})} + \|Q_r Q_p f - Q_r Q_0 f\|_{C^1(\overline{\Omega})} \\
 &\lesssim \left( \|Q_{r+1}\|_{C^1(\overline{\Omega})} + \|Q_r\|_{C^1(\overline{\Omega})} \right) \|Q_p f - Q_0 f\|_{C^1(\overline{\Omega})}
 \end{aligned}$$

which yields

$$\max_{l \leq p-1} \|\mathbf{d}_l\|_\infty \lesssim \|Q_p f - Q_0 f\|_{C^1(\overline{\Omega})}$$

because of Proposition 3.2. Using Lemma 3.5 the right inequality in (3.16) follows from

$$\|Q_p f - Q_0 f\|_{C^1(\overline{\Omega})} \leq \sum_{l=0}^{p-1} \|g_l\|_{C^1(\overline{\Omega})} \lesssim \sum_{l=0}^{p-1} \|\mathbf{d}_l\|_\infty. \quad \square$$

**4. Strong stability in the Sobolev spaces  $H^s(\Omega)$  with  $s \in (2, \frac{5}{2})$ .** In this section we prove that the multiscale basis  $\psi$  is a strongly stable basis for certain subspaces of the Banach space  $C^1(\overline{\Omega})$ , namely for the Sobolev spaces  $H^s(\Omega)$  with  $s \in (2, \frac{5}{2})$ . The outline of this section is as follows. First we give the definition of function spaces of Sobolev and Besov type. Then we prove Jackson and Bernstein type estimates for Powell–Sabin splines, using standard techniques developed in [15]. These estimates are crucial for the stability proof. Finally we show that the multiscale basis under a suitable normalization is strongly stable with respect to the norm in  $H^s(\Omega)$ ,  $s \in (2, \frac{5}{2})$ .

**4.1. Function spaces measuring smoothness.** We recall that Sobolev spaces measure the smoothness of a function  $f \in L_p(\Omega)$ . By  $W_p^m(\Omega)$ ,  $m \in \mathbb{N}$ ,  $1 \leq p \leq \infty$ , we mean the usual Sobolev space, i.e. the set of all functions in  $L_p(\Omega)$  whose distributional derivatives of order less than or equal to  $m$  are in  $L_p(\Omega)$ . We can define the following norm for these Banach spaces

$$\|f\|_{W_p^m(\Omega)}^p = \sum_{\alpha+\beta \leq m} \|D_x^\alpha D_y^\beta f\|_{L_p(\Omega)}^p,$$

with  $\alpha$  and  $\beta$  positive integers. We also use the semi-norm

$$|f|_{W_p^m(\Omega)}^p = \sum_{\alpha+\beta=m} \|D_x^\alpha D_y^\beta f\|_{L_p(\Omega)}^p.$$

For the special case  $p = 2$  we use the notation  $H^m(\Omega) \equiv W_2^m(\Omega)$ . These spaces  $H^m(\Omega)$  are Hilbert spaces with inner product

$$\langle f, g \rangle_{H^m(\Omega)} = \sum_{\alpha+\beta \leq m} \langle D_x^\alpha D_y^\beta f, D_x^\alpha D_y^\beta g \rangle_{L_2(\Omega)}.$$

We also define spaces  $W_p^s(\Omega)$  for arbitrary real values of  $s \geq 0$  and  $1 < p < \infty$ . These spaces coincide for integer values of  $s$  with the spaces  $W_p^m(\Omega)$ . If  $s$  is not an integer, we write  $s = m + \sigma$  where  $m$  is an integer and  $0 < \sigma < 1$ . Then  $W_p^s(\Omega)$  is a Banach space with respect to the norm

$$\|f\|_{W_p^s(\Omega)}^p = \|f\|_{W_p^m(\Omega)}^p + \sum_{\alpha+\beta=m} \int_{\Omega} \int_{\Omega} \frac{|D_x^\alpha D_y^\beta f(x) - D_x^\alpha D_y^\beta f(y)|^p}{|x - y|^{2+\sigma p}} dx dy.$$

Again for the special case  $p = 2$  we write  $H^s(\Omega) \equiv W_2^s(\Omega)$  and the spaces  $H^s(\Omega)$  are Hilbert spaces for arbitrary real values of  $s \geq 0$ . See [1] for a good reference work concerning Sobolev spaces.

Strongly related to Sobolev spaces are the function spaces of Besov type. Let  $f \in L_p(\Omega)$ ,  $0 < p \leq \infty$ . We introduce the difference operator

$$(\Delta_h^r f)(x) := \sum_{j=0}^r \binom{r}{j} (-1)^{r-j} f(x + jh), \quad x \in \mathbb{R}^2,$$

and define the  $r$ -th order  $L_p$ -modulus of smoothness of  $f \in L_p(\Omega)$  (see e.g. [14])

$$(4.1) \quad \omega_r(f, t)_p := \sup_{|h| \leq t} \|\Delta_h^r f\|_{L_p(\Omega(rh))},$$

where  $|h|$  is the Euclidean length of vector  $h$  and  $\Omega(rh) := \{x \in \Omega : x + jh \in \Omega, j = 0, \dots, r\}$ . The  $r$ -th order  $L_p$ -modulus of smoothness has the following properties

$$(4.2) \quad \begin{aligned} \omega_r(f, t)_p &\leq 2^r \|f\|_{L_p(\Omega)}, \\ \lim_{t \rightarrow 0^+} \omega_r(f, t)_p &= 0, \\ \omega_r(f + g, t) &\leq \omega_r(f, t)_p + \omega_r(g, t)_p. \end{aligned}$$

If  $s, p, q > 0$ , we say that  $f$  is in the Besov space  $B_q^s(L_p(\Omega))$  whenever the following is finite:

$$(4.3) \quad |f|_{B_q^s(L_p(\Omega))} \sim \begin{cases} (\sum_{l=0}^{\infty} [3^{ls} \omega_r(f, 3^{-l})_p]^q)^{1/q}, & 0 < q < \infty, \\ \sup_{l \geq 0} 3^{ls} \omega_r(f, 3^{-l})_p, & q = \infty. \end{cases}$$

See [14] for more details concerning Besov spaces.

It is well known that on a domain  $\Omega$  with Lipschitz boundary the equivalence

$$(4.4) \quad W_p^s(\Omega) \cong B_p^s(L_p(\Omega)), \quad s > 0$$

holds [17].

**4.2. Jackson and Bernstein type estimates for PS splines.** As mentioned before, the Jackson and Bernstein estimates for PS splines are proved by using techniques developed in [15]. More information on Jackson and Bernstein estimates can also be found in [5]. First we prove the Jackson type estimate. Let  $f \in L_p(\Omega)$ ,  $0 < p \leq \infty$ . We want to show that the local error of approximation by PS splines

$$(4.5) \quad E_l(f, \Omega)_p := \inf_{g \in S_l} \|f - g\|_{L_p(\Omega)}, \quad l \geq 0$$

can be bounded by  $E_l(f, \Omega)_p \lesssim \omega_3(f, 3^{-l})_p$ . From Whitney's theorem we know that the estimate

$$E_l(f, T)_p \lesssim \omega_3(f, 3^{-l})_p, \quad T \in \Delta_l^{PS}$$

holds, since  $g|_T$  is a quadratic polynomial for all  $g \in S_l$ . Whitney's theorem is best known for univariate functions and  $p \geq 1$  but a proof for multivariate functions and  $p > 0$  can be found in the papers [4] and [29].

Denote  $\Pi_2(\Delta_l^{PS})$  as the space of all piecewise polynomials of degree  $\leq 2$  on the triangulation  $\Delta_l^{PS}$ . Let  $\pi \in \Pi_2(\Delta_l^{PS})$ . Then  $Q_l \pi$  is not well defined because the operator  $Q_l$  evaluates the piecewise polynomial  $\pi$  and its partial derivatives at the vertices  $V_i \in \Delta_l$  and  $\pi$  may be discontinuous at  $V_i$ . Therefore we introduce a new operator  $Q_l^\circ$  as follows, let

$$(4.6) \quad Q_l^\circ f(x, y) := \sum_{i=1}^{N_l} \sum_{j=1}^3 \mu_{ij,l}^\circ(f) B_{ij,l}(x, y),$$

where the  $\mu_{ij,l}^\circ$  are linear functionals of the form

$$(4.7) \quad \mu_{ij,l}^\circ(f) := f^\circ(V_i) + \eta_{ij,l} D_x^\circ f(V_i) + \tilde{\eta}_{ij,l} D_y^\circ f(V_i),$$

with

$$(4.8) \quad \begin{cases} f^\circ(x) & := \limsup_{y \rightarrow x} f(y) \\ D_r^\circ f(x) & := \limsup_{y \rightarrow x, t \downarrow 0} \frac{f(y+tr) - f(y)}{t|r|} \end{cases}$$

Then we still have the property that  $Q_l^\circ s_l = s_l$  for each  $s_l \in S_l$ , but we also have that  $Q_l^\circ \pi$  is well defined.

LEMMA 4.1. *If  $\pi \in \Pi_2(\Delta_l^{PS})$  and  $0 < p \leq \infty$ , then for each triangle  $T \in \Delta_l^{PS}$  we have that*

$$(4.9) \quad \|Q_l^\circ \pi\|_{L_p(T)} \lesssim \|\pi\|_{L_p(M_T)}$$

and

$$(4.10) \quad \|\pi - Q_l^\circ \pi\|_{L_p(T)} \lesssim \inf_{P \in \mathcal{P}_2} \|\pi - P\|_{L_p(M_T)}$$

where  $\mathcal{P}_2$  is the space of bivariate polynomials of total degree  $\leq 2$  and  $M_T \subset \Omega$  satisfies  $T \subset M_T$  and  $|T| \sim |M_T|$ .

*Proof.* Because  $T \in \Delta_l^{PS}$  there is exactly one vertex  $V_i \in \Delta_l$  such that  $V_i \in T$ . Define  $M_T$  as the union of all triangles in  $\Delta_l^{PS}$  that contain vertex  $V_i$ . Then  $T \subset M_T$  and  $|T| \sim |M_T| \sim 3^{-l}$ . From Equations (2.12), (4.6)–(4.8) and the Markov inequality for polynomials we find that

$$\begin{aligned} \|Q_l^\circ \pi\|_{L_p(T)} &\lesssim \max_{\tilde{T} \subset M_T} \|\pi\|_{L_\infty(\tilde{T})} \left\| \sum_{i=1}^{N_l} \sum_{j=1}^3 B_{ij,l} \right\|_{L_p(T)} \\ &\lesssim \max_{\tilde{T} \subset M_T} 3^{2l/p} \|\pi\|_{L_p(\tilde{T})} \cdot 3^{-2l/p} \lesssim \|\pi\|_{L_p(M_T)} \end{aligned}$$

which is (4.9). Here we have also used that all norms on the finite dimensional space of polynomials are equivalent.

Now define  $P \in \mathcal{P}_2$  as the polynomial of best  $L_p(M_T)$  approximation to  $\pi$ . Since  $Q_l^\circ P = P$  we find that

$$\|\pi - Q_l^\circ \pi\|_{L_p(T)} \leq \|\pi - P\|_{L_p(T)} + \|Q_l^\circ(\pi - P)\|_{L_p(T)}$$

and by using (4.9) we find (4.10).  $\square$

Let  $f$  be in  $L_p(\Omega)$  and define for each triangle  $T \in \Delta_l^{PS}$  the polynomials  $P_T \in \mathcal{P}_2$  as the best  $L_p(T)$  approximation to  $f$ . Then we define  $\pi_l(f) \in \Pi_2(\Delta_l^{PS})$  to be the piecewise polynomial such that  $\pi_l(f)|_T := P_T$  for each triangle  $T \in \Delta_l^{PS}$ .

THEOREM 4.2. *For each  $f \in L_p(\Omega)$  we have*

$$(4.11) \quad \|f - Q_l^\circ \pi_l(f)\|_{L_p(\Omega)} \lesssim \omega_3(f, 3^{-l})_p, \quad l \geq 0.$$

*Proof.* For each  $T \in \Delta_l^{PS}$  we have from (4.10) that

$$\begin{aligned} \|f - Q_l^\circ \pi_l(f)\|_{L_p(T)} &\leq \|f - \pi_l(f)\|_{L_p(T)} + \|\pi_l(f) - Q_l^\circ \pi_l(f)\|_{L_p(T)} \\ &\lesssim \|f - P_T\|_{L_p(T)} + \inf_{P \in \mathcal{P}_2} \|\pi_l(f) - P\|_{L_p(M_T)}. \end{aligned}$$

The following equations hold:

$$\begin{aligned} \inf_{P \in \mathcal{P}_2} \|\pi_l(f) - P\|_{L_p(M_T)}^p &= \inf_{P \in \mathcal{P}_2} \sum_{\tilde{T} \subset M_T} \|P_{\tilde{T}} - P\|_{L_p(\tilde{T})}^p \\ &\lesssim \inf_{P \in \mathcal{P}_2} \sum_{\tilde{T} \subset M_T} \left( \|P_{\tilde{T}} - f\|_{L_p(\tilde{T})} + \|f - P\|_{L_p(\tilde{T})} \right)^p \\ &\lesssim \inf_{P \in \mathcal{P}_2} \sum_{\tilde{T} \subset M_T} \|f - P\|_{L_p(\tilde{T})}^p \\ &\lesssim \inf_{P \in \mathcal{P}_2} \|f - P\|_{L_p(M_T)}^p. \end{aligned}$$

So we infer that

$$(4.12) \quad \|f - Q_l^\circ \pi_l(f)\|_{L_p(T)} \lesssim \inf_{P \in \mathcal{P}_2} \|f - P\|_{L_p(M_T)}.$$

Now we make use of the fact that [15]

$$\omega_r(f, t)_p \sim \left( t^{-2} \int_{[-t, t]^2} \|\Delta_h^r f\|_{L_p(\Omega(rh))}^p dh \right)^{1/p}.$$

We deduce from (4.12) and Whitney's theorem that

$$\begin{aligned} \|f - Q_l^\circ \pi_l(f)\|_{L_p(\Omega)}^p &= \sum_{T \in \Delta_l^{PS}} \|f - Q_l^\circ \pi_l(f)\|_{L_p(T)}^p \\ &\lesssim \sum_{T \in \Delta_l^{PS}} |M_T|^{-2} \int_{[-|M_T|, |M_T|]^2} \|\Delta_h^r f\|_{L_p(M_T(rh))}^p dh \\ &\lesssim \max_{T \in \Delta_l^{PS}} |M_T|^{-2} \int_{[-|M_T|, |M_T|]^2} \|\Delta_h^r f\|_{L_p(\Omega(rh))}^p dh \end{aligned}$$

Equation (4.11) follows from the last inequality because  $\max_{T \in \Delta_l^{PS}} |M_T| \sim 3^{-l}$ .  $\square$

Theorem 4.2 immediately implies that the  $L_p$  error of approximation by Powell–Sabin splines is bounded by the modulus of smoothness, namely

COROLLARY 4.3 (Jackson estimate). *For each  $f \in L_p(\Omega)$ ,  $0 < p \leq \infty$ , we have that*

$$(4.13) \quad E_l(f, \Omega)_p \lesssim \omega_3(f, 3^{-l})_p.$$

Now we prove the Bernstein type estimate for Powell–Sabin splines.

THEOREM 4.4 (Bernstein estimate). *For each  $l \geq 0$ , each  $p > 0$ , and each  $r = 1, 2, 3$ , we have for  $\lambda := \min(r, r - 1 + \frac{1}{p})$  the Bernstein inequality*

$$(4.14) \quad \omega_r(g_l, t)_p \lesssim (\min\{1, 3^l t\})^\lambda \|g_l\|_{L_p(\Omega)}, \quad g_l \in S_l.$$

*Proof.* For  $t \geq 3^{-l}$  this inequality reduces to

$$\omega_r(g_l, t)_p \lesssim \|g_l\|_{L_p(\Omega)}$$

which follows directly from (4.2). We concentrate on  $t < 3^{-l}$ . From the definition of the operator  $Q_l$  (2.10) we can write

$$g_l(x, y) = Q_l g_l(x, y) = \sum_{i=1}^{N_l} \sum_{j=1}^3 \mu_{ij,l}(g_l) B_{ij,l}(x, y),$$

and also

$$(\Delta_h^r g_l)(x, y) = \sum_{i=1}^{N_l} \sum_{j=1}^3 \mu_{ij,l}(g_l) (\Delta_h^r B_{ij,l})(x, y).$$

For any  $(x, y) \in \Omega$  at most 9 B-splines are nonzero at  $(x, y)$ , hence

$$(4.15) \quad |(\Delta_h^r g_l)(x, y)|^p \leq 9 \sum_{i=1}^{N_l} \sum_{j=1}^3 |\mu_{ij,l}(g_l)|^p |(\Delta_h^r B_{ij,l})(x, y)|^p.$$

We shall give two estimates for  $|(\Delta_h^r B_{ij,l})(x, y)|$ . First define  $\Gamma_{ij,l}$  as the set of all  $(x, y)$  such that  $(x, y)$  and  $(x, y) + rh$  are in the same triangle  $T \in \Delta_l^{PS}$  and  $B_{ij,l}$  does not vanish identically on  $T$ . Then  $B_{ij,l}$  is a polynomial on  $T$  whose  $r$ -th order derivatives can be bounded by the Markov inequality for polynomials and we find that

$$(4.16) \quad |(\Delta_h^r B_{ij,l})(x, y)| \lesssim (3^l |h|)^r, \quad (x, y) \in \Gamma_{ij,l}.$$

The second estimate is for the set  $\tilde{\Gamma}_{ij,l}$  which consists of all  $(x, y)$  such that  $(x, y)$  and  $(x, y) + rh$  are in different triangles from  $\Delta_l^{PS}$  and  $B_{ij,l}$  does not vanish identically on both of these triangles. It is easy to see that  $B_{ij,l} \in W_\infty^{r-1}(\Omega)$ . Hence  $B_{ij,l}$  has  $(r-1)$ -th order derivatives whose  $L_\infty(\Omega)$  norms do not exceed  $C3^{l(r-1)}$ . We find that

$$(4.17) \quad |(\Delta_h^r B_{ij,l})(x, y)| \lesssim (3^l |h|)^{r-1}, \quad (x, y) \in \tilde{\Gamma}_{ij,l}.$$

The set  $\Gamma_{ij,l}$  has measure  $\lesssim (3^{-l})^2$  because the support of  $B_{ij,l}$  has measure  $\lesssim (3^{-l})^2$ , and a similar argument shows that  $\tilde{\Gamma}_{ij,l}$  has measure  $\lesssim |h|3^{-l}$ .

If we combine the estimates (4.16) and (4.17) with the estimates for the measures of  $\Gamma_{ij,l}$  and  $\tilde{\Gamma}_{ij,l}$  we obtain

$$(4.18) \quad \int_{\Omega(rh)} |(\Delta_h^r B_{ij,l})(x, y)|^p \lesssim (3^l |h|)^{pr} (3^{-l})^2 + (3^l |h|)^{p(r-1)} |h| 3^{-l} \\ \lesssim |h|^{p\lambda} 3^{pl\lambda} 3^{-2l}$$

where we have used that  $|h| \leq t < 3^{-l}$ .

We integrate (4.15) and use (4.18) to find

$$\|\Delta_h^r g_l\|_{L^p(\Omega(rh))}^p \lesssim \sum_{i=1}^{N_l} \sum_{j=1}^3 |\mu_{ij,l}(g_l)|^p |h|^{p\lambda} 3^{pl\lambda} 3^{-2l},$$

and because  $\sum_{i=1}^{N_l} \sum_{j=1}^3 3^{-2l} |\mu_{ij,l}(g_l)|^p \sim \|g_l\|_{L^p(\Omega)}^2$  (Theorem 2.1) we get

$$\|\Delta_h^r g_l\|_{L^p(\Omega(rh))}^p \lesssim (|h|3^l)^{p\lambda} \|g_l\|_{L^p(\Omega)}^p. \quad \square$$

REMARK 4.5. *Jackson and Bernstein estimates are properties of the spline space  $S_l$  itself, hence they do not depend on any underlying basis. Therefore, as in Remark 3.4, one can show these estimates using any basis for  $S_l$  that is stable in the sense of (2.13). See for instance [26] where Jackson and Bernstein estimates are derived for Powell–Sabin splines on a 12-split refinement using the Hermite basis [28].*

**4.3. Strong stability in  $H^s(\Omega)$ ,  $s \in (2, \frac{5}{2})$ .** We have shown that the operator  $Q_l$  from (2.10) is suitable for constructing a multiresolution analysis. This same operator will play a key role in proving strong stability.

LEMMA 4.6. *The Sobolev space  $H^s(\Omega)$  with  $s > 2$  is a subset of  $C^1(\overline{\Omega})$ . Therefore the operator  $Q_l$  is bounded on  $H^s(\Omega)$  with  $s > 2$ .*

*Proof.* Because  $\Omega$  is a bounded domain with polygonal boundary we have that  $\Omega$  satisfies the strong local Lipschitz property and the uniform cone property. From Theorems 5.4 and 7.58 in [1] the imbeddings

$$H^s(\Omega) \subset W_{2/(3-s)}^2 \subset C^1(\overline{\Omega})$$

hold for  $2 < s < 3$ . The case  $s = 3$  follows immediately from Theorem 5.4 in [1] and the case  $s > 3$  is obtained from the imbedding  $H^s(\Omega) \subset H^3(\Omega)$ . The boundedness of  $Q_l$  follows from Proposition 3.2.  $\square$

The operator  $Q_l$  is only useful if there exist function spaces for which  $Q_l f$  converges to  $f$  in some  $L_p$  norm as the resolution level  $l$  increases.

LEMMA 4.7. *For each  $f \in H^s(\Omega)$ ,  $s > 2$ , and arbitrary  $p > 0$  we have that*

$$\|f - Q_l f\|_{L_p(\Omega)} \rightarrow 0 \quad \text{as } l \rightarrow \infty.$$

*Proof.* We will only consider the case  $2 < s < 3$ . Let  $(x, y)$  be some arbitrary point in triangle  $T \in \Delta_l$ . From (3.9) we immediately get that

$$|f(x, y) - Q_l f(x, y)| \lesssim \|f\|_{L_\infty(T)} + 3^{-l} \|f\|_{C^1(\overline{T})}.$$

Then the well-known Bramble–Hilbert lemma [2] implies

$$|f(x, y) - Q_l f(x, y)| \lesssim (3^{-l})^{2-2/q} |f|_{W_q^2(T)}$$

for arbitrary  $q > 2$ . If we take  $q = 2/(3-s)$  then Theorem 7.58 in [1] yields  $H^s(T) \subset W_q^2(T)$  and so

$$|f(x, y) - Q_l f(x, y)| \lesssim 3^{-l(s-1)} |f|_{H^s(T)}.$$

By using (2.9) we find that

$$\begin{aligned} \|f - Q_l f\|_{L_p(T)} &= \left( \int_T |f(x, y) - Q_l f(x, y)|^p dx dy \right)^{1/p} \\ &\lesssim 3^{-l(s-1)} |f|_{H^s(T)} 3^{-2l/p}. \end{aligned}$$

Some elementary calculations then yield

$$\|f - Q_l f\|_{L_p(\Omega)} \lesssim 3^{-l(s-1+2/p)} |f|_{H^s(\Omega)}. \quad \square$$

From Lemma 4.7 we know that each function  $f \in H^s(\Omega)$ ,  $s > 2$ , can be decomposed as

$$f = \sum_{l=0}^{\infty} g_l, \quad g_l \in S_l,$$

in the sense of  $L_p$ . Moreover, we can use the decomposition

$$f = \sum_{l=0}^{\infty} (Q_l - Q_{l-1})f,$$

with  $Q_{-1} := 0$ .

We now introduce auxiliary spaces  $A_q^s(L_p(\Omega))$ . Under certain conditions these auxiliary spaces can be related to Besov spaces, which implies that the norm of an auxiliary space is equivalent to the norm of its corresponding Besov space. This important property is needed for proving stability.

**DEFINITION 4.8.** *A function  $f \in L_p(\Omega)$  belongs to  $A_q^s(L_p(\Omega))$  for some fixed  $s \geq 0$ ,  $1 \leq p, q \leq \infty$  if there exists a sequence  $g_l \in S_l$ ,  $l = 0, 1, \dots$  such that  $f = \sum_{l=0}^{\infty} g_l$  in the sense of  $L_p$ , and  $\|\{3^{ls}\|g_l\|_{L_p(\Omega)}\}\|_{l_q} < \infty$ . The norm on  $A_q^s(L_p(\Omega))$  is defined as*

$$\|f\|_{A_q^s(L_p(\Omega))} = \inf \left( \sum_{l=0}^{\infty} [3^{ls}\|g_l\|_{L_p(\Omega)}]^q \right)^{1/q}$$

where the infimum must be taken with respect to all admissible representations  $\sum_{l=0}^{\infty} g_l$  of  $f$ . So in order to work with the abstract  $A_q^s(L_p(\Omega))$ -spaces, we relate them to the more convenient function spaces of Besov type. The following fact can be extracted from the results in [26].

**PROPOSITION 4.9.** *Suppose the nested spaces  $\{S_l\}_{l=0}^{\infty}$  satisfy Jackson estimates (4.13) for all  $f \in L_p(\Omega)$ , as well as Bernstein estimates (4.14) for  $r = 3$ , then for  $1 \leq p, q \leq \infty$ ,  $s > 0$*

$$(4.19) \quad A_q^s(L_p(\Omega)) \cong B_q^s(L_p(\Omega)), \quad 0 < s < 2 + \frac{1}{p}.$$

If we take  $p = q = 2$  then Proposition 4.9 is not valid for  $s > \frac{5}{2}$ , so it reduces the range of Sobolev spaces  $H^s(\Omega)$  that are possibly stable from  $s > 2$  to  $s \in (2, \frac{5}{2})$  because the equivalence (4.19) is crucial for proving stability. Equation (4.4) and Proposition 4.9 yield

$$(4.20) \quad \|f\|_{H^s(\Omega)}^2 \sim \inf_{g_l \in S_l: f = \sum_l g_l} \sum_{l=0}^{\infty} 3^{2ls} \|g_l\|_{L_2(\Omega)}^2, \quad 0 < s < \frac{5}{2}.$$

Using the norm equivalence (4.20) we can now prove the following theorem which is inspired by the work in [11] and [12]. This theorem is the most important step in proving stability in  $H^s(\Omega)$ .

**THEOREM 4.10.** *Choose  $s \in (2, \frac{5}{2})$ . Then it holds that*

$$(4.21) \quad \|f\|_{H^s(\Omega)}^2 \sim \sum_{l=0}^{\infty} 3^{2ls} \|(Q_l - Q_{l-1})f\|_{L_2(\Omega)}^2, \quad f \in H^s(\Omega).$$

*Proof.* Because of the norm equivalence (4.20) it is sufficient to prove that

$$\inf_{g_l \in S_l: f = \sum_l g_l} \sum_{l=0}^{\infty} 3^{2ls} \|g_l\|_{L_2(\Omega)}^2 \sim \sum_{l=0}^{\infty} 3^{2ls} \|(Q_l - Q_{l-1})f\|_{L_2(\Omega)}^2.$$

Since  $(Q_l - Q_{l-1})f \in S_l$  and  $\sum_{l=0}^{\infty} (Q_l - Q_{l-1})f = f$  the inequality “ $\lesssim$ ” is trivial and we will concentrate on the inequality “ $\gtrsim$ ”. Let  $f = \sum_{l=0}^{\infty} g_l$  with  $g_l \in S_l$ . Since the operators  $Q_l$  are projectors and the spaces  $S_l$  are nested, we have  $(Q_l - Q_{l-1})S_n = 0$  when  $n \leq l - 1$ . Moreover the operators  $Q_l$  also satisfy

$$(4.22) \quad \|Q_l s_n\|_{L_2(\Omega)} \lesssim 3^{2(n-l)} \|s_n\|_{L_2(\Omega)}, \quad s_n \in S_n.$$

Indeed, from (2.11), (2.12), (3.5) and the Markov inequality (3.7) we get

$$\|Q_l s_n\|_{L_\infty(\Omega)} \lesssim \|s_n\|_{L_\infty(\Omega)} + 3^{-l} 3^n \|s_n\|_{L_\infty(\Omega)} \lesssim 3^{n-l} \|s_n\|_{L_\infty(\Omega)}.$$

Then (4.22) can be deduced by using (2.13) and (2.14).

From the properties above and the Cauchy–Schwartz inequality we have

$$\begin{aligned} & \sum_{n,n'=0}^{\infty} \sum_{l=0}^{\infty} 3^{2ls} \langle (Q_l - Q_{l-1})g_n, (Q_l - Q_{l-1})g_{n'} \rangle_{L_2(\Omega)} \\ &= \sum_{n,n'=0}^{\infty} \sum_{l=0}^{\min\{n,n'\}} 3^{2ls} \langle (Q_l - Q_{l-1})g_n, (Q_l - Q_{l-1})g_{n'} \rangle_{L_2(\Omega)} \\ &\leq \sum_{n,n'=0}^{\infty} \sum_{l=0}^{\min\{n,n'\}} 3^{2ls} (\|Q_l g_n\|_{L_2(\Omega)} + \|Q_{l-1} g_n\|_{L_2(\Omega)}) \\ &\quad \cdot (\|Q_l g_{n'}\|_{L_2(\Omega)} + \|Q_{l-1} g_{n'}\|_{L_2(\Omega)}) \\ &\lesssim \sum_{n,n'=0}^{\infty} \sum_{l=0}^{\min\{n,n'\}} 3^{2ls} 3^{2(n+n')-4l} \|g_n\|_{L_2(\Omega)} \|g_{n'}\|_{L_2(\Omega)}. \end{aligned}$$

The last expression can be rewritten as

$$\sum_{n,n'=0}^{\infty} \sum_{l=0}^{\min\{n,n'\}} 3^{(s-2)(2l-n-n')} (3^{ns} \|g_n\|_{L_2(\Omega)}) (3^{n's} \|g_{n'}\|_{L_2(\Omega)}),$$

which is equivalent to

$$\sum_{n,n'=0}^{\infty} 3^{(s-2)(2\min\{n,n'\}-n-n')} (3^{ns} \|g_n\|_{L_2(\Omega)}) (3^{n's} \|g_{n'}\|_{L_2(\Omega)}).$$

The factor  $3^{(s-2)(2\min\{n,n'\}-n-n')}$  becomes very small if  $|n - n'| \gg 0$ . In fact, the infinite matrix  $[3^{(s-2)(2\min\{n,n'\}-n-n')}]_{n,n' \in \mathbb{N}}$  defines a bounded mapping on  $l_2$ . Therefore

$$\sum_{n,n'=0}^{\infty} 3^{(s-2)(2\min\{n,n'\}-n-n')} (3^{ns} \|g_n\|_{L_2(\Omega)}) (3^{n's} \|g_{n'}\|_{L_2(\Omega)}) \lesssim \sum_{n=0}^{\infty} 3^{2ns} \|g_n\|_{L_2(\Omega)}^2.$$

Since the splitting  $f = \sum_{l=0}^{\infty} g_l$  was arbitrary, we have derived that

$$\begin{aligned} & \inf_{g_l \in S_l: f = \sum_l g_l} \sum_{n,n'=0}^{\infty} \sum_{l=0}^{\infty} 3^{2ls} \langle (Q_l - Q_{l-1})g_n, (Q_l - Q_{l-1})g_{n'} \rangle_{L_2(\Omega)} \\ &\lesssim \inf_{g_l \in S_l: f = \sum_l g_l} \sum_{n=0}^{\infty} 3^{2ns} \|g_n\|_{L_2(\Omega)}^2. \end{aligned}$$

Because  $f \in A_2^s(L_2(\Omega))$  (Proposition 4.9) we know that the right expression is bounded. Then from the derivation made above it follows that the left expression is absolutely conver-

gent and we are allowed to write that

$$\begin{aligned}
 & \inf_{g_l \in S_l: f = \sum_l g_l} \sum_{n, n'=0}^{\infty} \sum_{l=0}^{\infty} 3^{2ls} \langle (Q_l - Q_{l-1})g_n, (Q_l - Q_{l-1})g_{n'} \rangle_{L_2(\Omega)} \\
 &= \inf_{g_l \in S_l: f = \sum_l g_l} \sum_{l=0}^{\infty} \sum_{n, n'=0}^{\infty} 3^{2ls} \langle (Q_l - Q_{l-1})g_n, (Q_l - Q_{l-1})g_{n'} \rangle_{L_2(\Omega)} \\
 &= \sum_{l=0}^{\infty} 3^{2ls} \|(Q_l - Q_{l-1})f\|_{L_2(\Omega)}^2.
 \end{aligned}$$

We conclude that

$$\sum_{l=0}^{\infty} 3^{2ls} \|(Q_l - Q_{l-1})f\|_{L_2(\Omega)}^2 \lesssim \inf_{g_l \in S_l: f = \sum_l g_l} \sum_{l=0}^{\infty} 3^{2ls} \|g_l\|_{L_2(\Omega)}^2. \quad \square$$

Proving that the basis  $\bigcup_{l=0}^{\infty} \{3^{-sl}\psi_{l-1}\}$  is a strongly stable basis for  $H^s(\Omega)$  with  $2 < s < \frac{5}{2}$  involves only a few steps now.

**COROLLARY 4.11.** *The multiscale basis  $\bigcup_{l=0}^{\infty} \{3^{-sl}\psi_{l-1}\}$  is a strongly stable basis for  $H^s(\Omega)$ ,  $2 < s < \frac{5}{2}$ .*

*Proof.* Since the wavelets  $\psi_l$  form a  $L_2$ -stable Riesz basis for  $W_l$  we find from Theorem 4.10 that

$$\begin{aligned}
 \|f\|_{H^s(\Omega)}^2 &\sim \sum_{l=-1}^{\infty} 3^{2(l+1)s} \left\| \sum_{m \in J_l} d_{l,m} \psi_{l,m} \right\|_{L_2(\Omega)}^2 \\
 &\sim \sum_{l=-1}^{\infty} 3^{2(l+1)s} \sum_{m \in J_l} |d_{l,m}|^2.
 \end{aligned}$$

Hence,

$$\left\| \sum_{l=-1}^{\infty} \sum_{m \in J_l} d_{l,m} 3^{-s(l+1)} \psi_{l,m} \right\|_{H^s(\Omega)}^2 \sim \sum_{l=-1}^{\infty} \sum_{m \in J_l} |d_{l,m}|^2. \quad \square$$

**5. Surface compression.** In the previous sections we have sufficiently demonstrated that Powell–Sabin wavelet decompositions are suitable for surface compression. We have proved that the norm of  $f$  in several smoothness classes can be determined from the size of the coefficients in the wavelet decomposition. In this section we consider a simple surface compression algorithm and we give an error bound for the approximation of  $f$  by its compressed wavelet decomposition. The most natural norm for compression is the  $L_{\infty}$  norm, so our approximation results take place in this norm. These results are obtained by following the framework given in [13] and adapted to the special case of PS splines.

**5.1. The algorithm.** Not all functions  $f$  are suitable for compression by Powell–Sabin splines. If we use the operator  $Q_l$  to project given functions  $f$  into  $S_l$ , then we need at least that the gradient  $\nabla f$  is well defined at the vertices  $V_i \in \Delta_l$ . However we would also like to compress continuous functions  $f$  for which  $Q_l f$  might not be well defined. Therefore we construct a new operator  $Q_l^{\nabla}$  that only uses values of the given function  $f$ . It suffices to approximate the gradient  $\nabla f(V_i)$  by a linear combination of values of  $f$  such that the

approximation is exact for quadratic polynomials. Let  $V_i$ ,  $R_i$  and  $Z_i$  denote the vertices of a triangle  $T \in \Delta_l^{PS}$  as in Figure 5.1. Then we can estimate the gradient  $\nabla f(V_i)$  by

$$(5.1) \quad \nabla_l f(V_i) := \begin{bmatrix} R_i^x - V_i^x & R_i^y - V_i^y \\ Z_i^x - V_i^x & Z_i^y - V_i^y \end{bmatrix}^{-1} \begin{bmatrix} 4f(\frac{V_i+R_i}{2}) - 3f(V_i) - f(R_i) \\ 4f(\frac{V_i+Z_i}{2}) - 3f(V_i) - f(Z_i) \end{bmatrix}$$

and because  $s_l \in S_l$  is a quadratic polynomial on each triangle  $T \in \Delta_l^{PS}$  we find that

$$(5.2) \quad \nabla s(V_i) = \nabla_l s(V_i).$$

Note that

$$\begin{bmatrix} R_i^x - V_i^x & R_i^y - V_i^y \\ Z_i^x - V_i^x & Z_i^y - V_i^y \end{bmatrix}^{-1} = \frac{1}{\text{vol}(T)} \begin{bmatrix} Z_i^y - V_i^y & V_i^y - R_i^y \\ V_i^x - Z_i^x & R_i^x - V_i^x \end{bmatrix}$$

which yields

$$(5.3) \quad |\nabla_l f(V_i)| \lesssim 3^l \|f\|_{L_\infty(T)}.$$

Thus we define the operator  $Q_l^\nabla$  analogous to the operator  $Q_l$  from (2.10) with the minor modification that we replace  $\nabla f(V_i)$  by the approximation  $\nabla_l f(V_i)$ . Because of (5.2) it is easy to see that the operators  $Q_l^\nabla$  satisfy  $Q_l^\nabla s_l = s_l$  and

$$Q_l^\nabla f(V_i) = f(V_i), \quad \nabla Q_l^\nabla f(V_i) = \nabla_l f(V_i), \quad i = 1, \dots, N_l.$$

Furthermore, from (5.3) we find that  $|Q_l^\nabla f(x, y)| \lesssim \|f\|_{L_\infty(\Omega)}$  for arbitrary  $(x, y) \in \Omega$ , so the operator  $Q_l^\nabla$  is uniformly bounded in  $C^0(\bar{\Omega})$ .

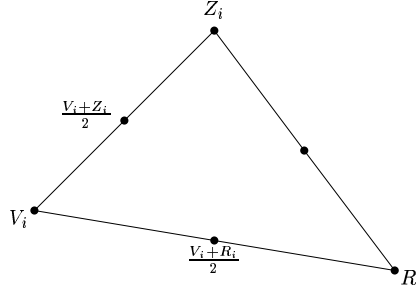


FIG. 5.1. A triangle  $T \in \Delta_l^{PS}$  that contains vertex  $V_i \in \Delta_l$ .

Still not all functions  $f$  are suitable for compression by Powell–Sabin splines. We need at least that the functions are  $C^0$  such that  $Q_l^\nabla f$  is well defined. Furthermore we would like that  $f$  can be represented as

$$(5.4) \quad f = \sum_{l=-1}^{\infty} \sum_{m \in J_l} d_{m,l} \psi_{m,l}$$

with convergence in  $L_\infty$ . Therefore we are particularly interested in functions  $f$  lying in Besov spaces that are embedded in  $B_\infty^\delta(L_\infty(\Omega)) = \text{Lip}(\delta, \Omega)$  for  $\delta > 0$ . For the remainder of the paper we define  $\tau := \frac{2}{s}$  and  $\delta := \frac{2}{\tau} - \frac{2}{\sigma}$  for some  $\sigma \geq 0$ .

LEMMA 5.1. *Let  $s > 0$  and  $\sigma > \tau$ , then*

$$B_\sigma^s(L_\sigma(\Omega)) \subset B_\infty^\delta(L_\infty(\Omega)) = \text{Lip}(\delta, \Omega).$$

*Proof.* The case  $\sigma \geq 1$  follows immediately from Theorems 7.69 and 7.70 in [1]. For the case  $\sigma < 1$  we can use Theorems 12.3, 12.5 and 12.7 from [16].  $\square$

Lemma 5.1 guarantees that  $Q_l^\nabla f$  is well defined for all  $f \in B_\sigma^s(L_\sigma(\Omega))$  given that  $\sigma > \tau$ . The following corollary validates the representation (5.4) with convergence in  $L_\infty$  for all  $f \in B_\sigma^s(L_\sigma(\Omega)), \sigma > \tau$ .

**COROLLARY 5.2.** *For all  $f \in B_\sigma^s(L_\sigma(\Omega))$  with  $s < 3$ , all  $\sigma > \tau$ , and arbitrary  $l \geq 0$  we have that*

$$\|f - Q_l^\nabla f\|_{L_\infty(\Omega)} \lesssim 3^{-\delta l} |f|_{B_\sigma^s(L_\sigma(\Omega))}.$$

*Proof.* Since  $Q_l^\nabla$  is bounded on  $C^0(\overline{\Omega})$  we find that

$$\begin{aligned} \|f - Q_l^\nabla f\|_{L_\infty(\Omega)} &\leq \inf_{g \in S_l} \left( \|f - g\|_{L_\infty(\Omega)} + \|Q_l^\nabla(g - f)\|_{L_\infty(\Omega)} \right) \\ &\leq \left( 1 + \|Q_l^\nabla\|_{L_\infty(\Omega)} \right) \inf_{g \in S_l} \|f - g\|_{L_\infty(\Omega)} \\ &\lesssim \inf_{g \in S_l} \|f - g\|_{L_\infty(\Omega)} \end{aligned}$$

and from Corollary 4.3

$$(5.5) \quad \|f - Q_l^\nabla f\|_{L_\infty(\Omega)} \lesssim \omega_3(f, 3^{-l})_\infty.$$

By (4.3) and Lemma 5.1 we know that

$$3^{\delta l} \omega_3(f, 3^{-l})_\infty \lesssim |f|_{B_\infty^s(L_\infty(\Omega))} \lesssim |f|_{B_\sigma^s(L_\sigma(\Omega))}. \quad \square$$

Suppose we are given a function  $f \in B_\sigma^s(L_\sigma(\Omega)), \sigma > \tau$  that represents the surface that is being compressed. The surface compression algorithm is as follows.

**Surface compression algorithm**

Let  $K$  be such that  $f \approx Q_K^\nabla f$ , then we obtain the decomposition

$$f \approx \sum_{l=-1}^{K-1} \sum_{m \in J_l} d_{m,l} \psi_{m,l}.$$

At all levels  $l \geq -1$  we only retain those coefficients  $d_{m,l}$  that satisfy  $|d_{m,l}| > \epsilon_l$  with  $\epsilon_l$  a threshold given by (5.8).

**5.2. A priori error bounds.** We will need some estimation for the constant  $K$ , i.e. the maximum number of resolution levels. Suppose we are looking for a compressed approximant  $S$  of  $f$  such that

$$\|f - S\|_{L_\infty(\Omega)} \leq \epsilon.$$

Corollary 5.2 gives us an a priori bound for the number of resolution levels. Choose  $K$  such that

$$(5.6) \quad \|f - Q_K^\nabla f\|_{L_\infty(\Omega)} \leq \epsilon/2,$$

then we find that

$$(5.7) \quad K \geq \frac{1}{\delta \log 3} \log \left( \frac{2C \|f\|_{B_\sigma^s(L_\sigma(\Omega))}}{\epsilon} \right)$$

where  $C$  is the equivalence constant in Corollary 5.2.

From (2.15) we find that

$$\sum_{m \in J_l} |\psi_{m,l}| = \|\psi_l\|_1 \leq \|\phi_{l+1}\|_1 = 3^l.$$

If we retain only the coefficients  $d_{m,l}$  of  $Q_K^\nabla f$  that satisfy  $|d_{m,l}| > \epsilon_l$  with

$$(5.8) \quad \epsilon_l = \frac{\epsilon}{2(K+1)3^l},$$

then

$$(5.9) \quad \|Q_K^\nabla f - S\|_{L_\infty(\Omega)} \leq \epsilon/2$$

because the maximal error is given by

$$\sum_{l=-1}^{K-1} \sum_{m \in J_l} \epsilon_l \psi_{m,l} \leq \frac{\epsilon}{2(K+1)} \sum_{l=-1}^{K-1} \sum_{m \in J_l} \frac{|\psi_{m,l}|}{3^l} \leq \frac{\epsilon}{2}.$$

From (5.6) and (5.9) we deduce that

$$(5.10) \quad \|f - S\|_{L_\infty(\Omega)} \leq \|f - Q_K^\nabla f\|_{L_\infty(\Omega)} + \|Q_K^\nabla f - S\|_{L_\infty(\Omega)} \leq \epsilon.$$

We will now examine the coefficients  $d_{m,l}$ . We have that

$$(Q_{l+1} - Q_l)Q_K^\nabla f = \sum_{m \in J_l} d_{m,l} \psi_{l,m},$$

and from (2.9), the construction of the projectors  $Q_l$ , and the fact that the wavelets are scaling functions at a certain resolution level, we infer

$$|d_{m,l}| \lesssim 3^{-l} \|Q_K^\nabla f\|_{L_\infty(T_m)} \sim 3^{-l} \|f\|_{L_\infty(T_m)}$$

with  $T_m$  a triangle in  $\Delta_l^{PS}$  such that  $\text{supp } \psi_{m,l} \cap T_m \neq \emptyset$ . Now let  $\pi \in \mathcal{P}_2$  be an arbitrary bivariate polynomial of degree at most 2. Then

$$(Q_{l+1} - Q_l)Q_K^\nabla f = (Q_{l+1} - Q_l)(Q_K^\nabla f - \pi),$$

so we also find that

$$|d_{m,l}| \lesssim 3^{-l} \inf_{\pi \in \mathcal{P}_2} \|f - \pi\|_{L_\infty(T_m)}$$

The following lemma gives an upper bound for the coefficients  $d_{m,l}$  in function of  $|f|_{B_\sigma^s(L_\sigma(\Omega))}$ .

LEMMA 5.3. *Let  $s < 3$  and let  $f \in B_\sigma^s(L_\sigma(\Omega))$ . Then the coefficients  $d_{m,l}$  in the decomposition (5.4) satisfy*

$$(5.11) \quad |d_{m,l}| \lesssim 3^{-l(\delta+1)} |f|_{B_\sigma^s(L_\sigma(T_m))}$$

for all  $\sigma > \tau$ .

*Proof.* From the derivation above and Whitney's Theorem we infer

$$|d_{m,l}| \lesssim 3^{-l} \omega_3(f, 3^{-l})_\infty,$$

and the same reasoning as in the proof of Corollary 5.2 yields

$$|d_{m,l}| \lesssim 3^{-l(\delta+1)} |f|_{B_\sigma^s(L_\sigma(T_m))}. \quad \square$$

We now give a bound for the number of terms  $N$  in the compressed approximant  $S$  such that the error remains bounded by the threshold  $\epsilon$ .

THEOREM 5.4. *Let  $f$  be a function in  $B_\sigma^s(L_\sigma(\Omega))$  with  $s < 3$  and such that  $|f|_{B_\sigma^s(L_\sigma(\Omega))} \leq 1$  for some  $\sigma > \tau$ . Then our surface compression algorithm provides an approximation  $S$  such that*

$$(5.12) \quad \|f - S\|_{L_\infty(\Omega)} \leq \epsilon$$

and

$$(5.13) \quad N \leq C \epsilon^{-2/s}$$

where  $N$  represents the number of terms in  $S$ .

*Proof.* Note that the bound for  $K$  (5.7) does not depend on  $f$  anymore. We already know that (5.12) is true, see (5.10). Let  $N_l$  denote the number of terms at resolution level  $l$ , then a trivial bound for  $N_l$  is

$$(5.14) \quad N_l \lesssim 9^l$$

which follows from the fact that we have used triadic refinement to create the nested subspaces  $\{S_l\}_{l=0}^\infty$ . We give another bound for  $N_l$ . We know that each coefficient  $d_{m,l}$  in  $S$  satisfies  $|d_{m,l}| > \epsilon_l$  but we have also the upper bound (5.11). If we raise  $d_{m,l}$  to the power  $\sigma$  and sum over all  $m \in J_l$  then we obtain that

$$\begin{aligned} N_l \left( \frac{\epsilon}{2(K+1)3^l} \right)^\sigma &< \sum_{m \in J_l} |d_{m,l}|^\sigma \lesssim \sum_{m \in J_l} 3^{-\sigma l(\delta+1)} |f|_{B_\sigma^s(L_\sigma(T_m))}^\sigma \\ &\lesssim 3^{-\sigma l(\delta+1)} |f|_{B_\sigma^s(L_\sigma(\Omega))}^\sigma. \end{aligned}$$

Under the assumption  $|f|_{B_\sigma^s(L_\sigma(\Omega))} \leq 1$  we find

$$(5.15) \quad N_l \lesssim \epsilon^{-\sigma} 3^{-\sigma l \delta}.$$

From (5.14) and (5.15) we find for an arbitrary integer  $k$  that

$$N \lesssim \sum_{l=1}^k 9^l + \sum_{l=k}^K \epsilon^{-\sigma} 3^{-\sigma l \delta} \lesssim 9^k + \epsilon^{-\sigma} 3^{-\sigma k \delta}.$$

Choose  $k$  such that  $9^k \approx \epsilon^{-\sigma} 3^{-\sigma k \delta}$ , then  $N \lesssim 9^k$ . Furthermore we deduce that  $9^k 3^{\sigma k \delta} = 3^{2k(1+\frac{\sigma \delta}{2})} \approx \epsilon^{-\sigma}$  and that  $9^k \approx \epsilon^{-\sigma} / (1 + \frac{\sigma \delta}{2}) = \epsilon^{-2/s}$ , so

$$N \lesssim 9^k \approx \epsilon^{-2/s}. \quad \square$$

The following corollary is the main result of this section. It is a direct consequence of Theorem 5.4.

**COROLLARY 5.5.** *If  $f \in B_\sigma^s(L_\sigma(\Omega))$  with  $s < 3$ , and  $N \in \mathbb{N}$  are given, then one can choose the threshold  $\epsilon$  and the maximum resolution level  $K$  such that the compression algorithm generates an approximant  $S$  to  $f$  with at most  $N$  terms and*

$$\|f - S\|_{L_\infty(\Omega)} \lesssim |f|_{B_\sigma^s(L_\sigma(\Omega))} N^{-s/2}$$

for arbitrary  $\sigma > \tau$ .

*Proof.* This proof is the same as the proof of Corollary 5.4 in [13] but we give it here for completeness. Let  $\epsilon := C^{s/2} N^{-s/2} |f|_{B_\sigma^s(L_\sigma(\Omega))}$  with  $C$  the constant from (5.13). If we apply the algorithm to  $f$  and  $\epsilon$  we get a compressed approximant  $S$ . If we apply the algorithm to  $\frac{f}{|f|_{B_\sigma^s(L_\sigma(\Omega))}}$  and  $\frac{\epsilon}{|f|_{B_\sigma^s(L_\sigma(\Omega))}}$  then the algorithm returns  $\frac{S}{|f|_{B_\sigma^s(L_\sigma(\Omega))}}$  as compressed approximant. From Theorem 5.4 the number of terms in  $S$  does not exceed  $C \left( \frac{\epsilon}{|f|_{B_\sigma^s(L_\sigma(\Omega))}} \right)^{-2/s}$  which is equal to  $N$ .  $\square$

**5.3. Numerical experiments.** We can compare the error bound for the compressed approximant  $S$  of  $f$  to an error bound for the linear approximant  $Q_l^\nabla f$ . If each approximation has  $N$  coefficients then we have that

$$(5.16) \quad \|f - S\|_{L_\infty(\Omega)} \lesssim N^{-s/2} |f|_{B_\sigma^s(L_\sigma(\Omega))}, \quad s < 3,$$

and

$$(5.17) \quad \|f - Q_l^\nabla f\|_{L_\infty(\Omega)} \lesssim N^{-s/2} |f|_{B_\infty^s(L_\infty(\Omega))}, \quad s < 3,$$

for all  $f \in B_\sigma^s(L_\sigma(\Omega))$  and for all  $\sigma > \tau$ . The error bound for  $Q_l^\nabla f$  follows immediately from Corollary 5.2 and  $N \sim 9^l$ . These error bounds (5.16) and (5.17) show that  $\|f - S\|_{L_\infty(\Omega)} = \mathcal{O}(N^{-s/2})$  if  $f$  has  $s$  “derivatives” in  $L_\sigma$  while  $\|f - Q_l^\nabla f\|_{L_\infty(\Omega)} = \mathcal{O}(N^{-s/2})$  if  $f$  has  $s$  “derivatives” in  $L_\infty$  which is a much stricter requirement. It can often happen that the right hand side of (5.16) is finite for certain values of  $s$  for which the right hand side of (5.17) is infinite.

To demonstrate the accuracy of the error bounds we performed experiments with several test functions. In all cases we choose  $\Delta_0$  as the triangulation that is constructed by dividing the unit square  $[0, 1]^2 \in \mathbb{R}^2$  by its bisector in two triangles. We selected the following

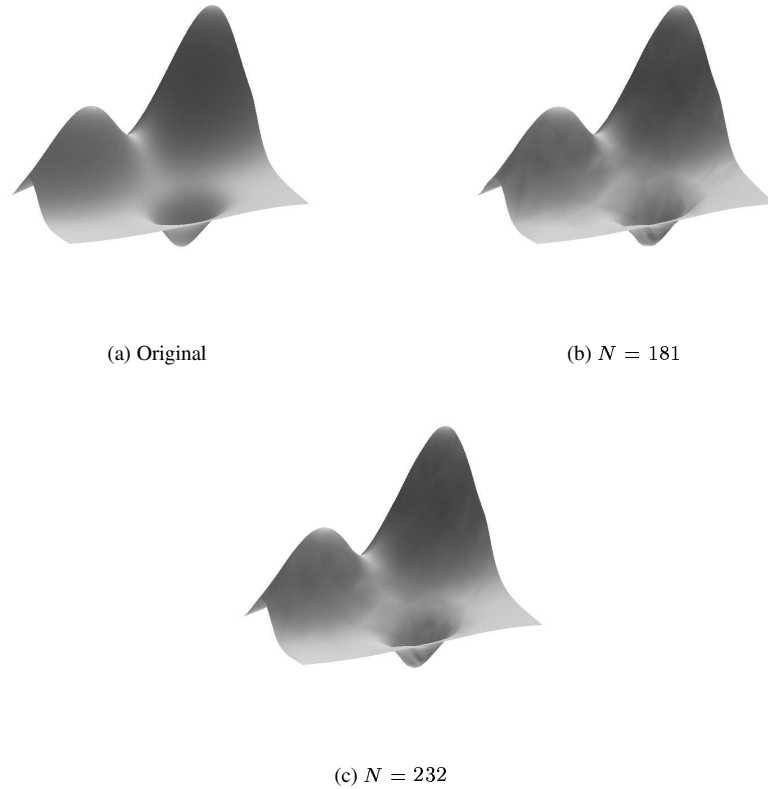


FIG. 5.2. Test function  $f_1$ .

bivariate test functions given by

$$\begin{aligned}
 f_1(x, y) &= 0.75 \exp \left[ -\frac{(9x-2)^2 + (9y-2)^2}{4} \right] + 0.75 \exp \left[ -\frac{(9x+1)^2}{49} - \frac{(9y+1)^2}{10} \right] \\
 &\quad + 0.5 \exp \left[ -\frac{(9x-7)^2 + (9y-3)^2}{4} \right] - 0.2 \exp \left[ -(9x-4)^2 - (9y-7)^2 \right], \\
 f_2(x, y) &= 9(x-y) \left( \exp \left[ -\frac{1}{9} ((x-y)^2)^{1/8} \right] - 1 \right), \\
 f_3(x, y) &= 97(x-0.5) \tanh \left[ \frac{1}{97} ((x-0.5)^2 + (y-0.5)^2)^{1/4} \right], \\
 f_4(x, y) &= \exp[-|x-y|], \\
 f_5(x, y) &= ((2x-1)^2 + (2y-1)^2)^{1/4}.
 \end{aligned}$$

Function  $f_1$  is Franke's test function [21] and it is smooth everywhere. Function  $f_2$  is  $C^1$  but its partial derivatives have singularities on the line  $y = x$ . Function  $f_3$  is also  $C^1$  but its partial derivatives have a cusp singularity at  $(1/2, 1/2)$ . Function  $f_4$  is only Lipschitz continuous and it has singularities on the line  $y = x$ . And finally function  $f_5$  is  $C^0$  (not Lipschitz) with a cusp singularity at  $(1/2, 1/2)$ . Because the error bound (5.16) is valid for all Besov spaces  $B_\sigma^s(L_\sigma(\Omega))$  as long as  $\sigma > \tau$  we will base our discussion on the Besov

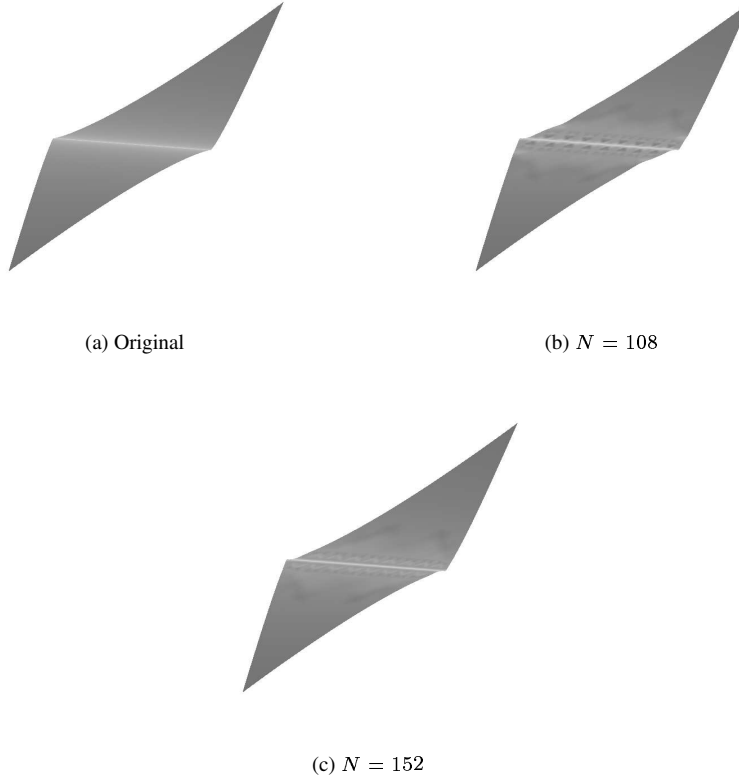


FIG. 5.3. Test function  $f_2$ .

spaces  $B_\tau^s(L_\tau(\Omega))$  which are close to  $B_\sigma^s(L_\sigma(\Omega))$  (take  $\sigma = \tau + \epsilon$  and let  $\epsilon \rightarrow 0_+$ ).

For the function  $f_1$  we do not expect much advantage from the compressed approximant to the linear approximant. Because  $f_1$  is  $C^\infty$  the norms  $|f_1|_{B_\sigma^s(L_\sigma(\Omega))}$  and  $|f_1|_{B_\infty^s(L_\infty(\Omega))}$  are comparable for all  $\sigma > 0$ .

For the function  $f_2$  we compute that  $|(\Delta_h^3 f_2)(x, y)| \approx |h|^{5/4}$  in a band of width  $|h|$  along the line  $y = x$ . It follows that

$$\omega_3(f_2, t)_\tau \approx t^{5/4+1/\tau}, \quad 0 < t < 1, \quad 0 < \tau \leq \infty.$$

Therefore we have that  $f_2 \in B_\tau^s(L_\tau(\Omega))$  provided that  $s < \frac{5}{2}$  while  $f_2 \in B_\infty^s(L_\infty(\Omega))$  provided  $s < \frac{5}{4}$ .

The 3-th order difference  $|(\Delta_h^3 f_3)(x, y)|$  is approximately equal to  $|h^{3/2}|$  in a disc with diameter  $|h|$  around  $(1/2, 1/2)$ . This yields  $\omega_3(f_3, t)_\tau \approx t^{3/2+2/\tau}$  and  $f_3 \in B_\tau^s(L_\tau(\Omega))$  for all  $s < 3$  while  $f_3 \in B_\infty^s(L_\infty(\Omega))$  provided  $s < \frac{3}{2}$ .

The function  $f_4$  has singularities along the line  $y = x$  and similar computations as before yield  $\omega_3(f_4, t)_\tau \approx t^{1+1/\tau}$ . Therefore the function  $f_4$  is in  $B_\tau^s(L_\tau(\Omega))$  provided that  $s < 2$  and  $f_4$  is in  $B_\infty^s(L_\infty(\Omega))$  for  $s < 1$ .

The last function  $f_5$  has a cusp singularity in  $(1/2, 1/2)$  and the modulus of smoothness  $\omega_3(f_5, t)_\tau \approx t^{1/2+2/\tau}$ . Therefore the function  $f_5$  is in all of the spaces  $B_\sigma^s(L_\sigma(\Omega))$  for all  $s < 3$ , while  $f_5$  is in the spaces  $B_\infty^s(L_\infty(\Omega))$  only for  $s < 1/2$ .

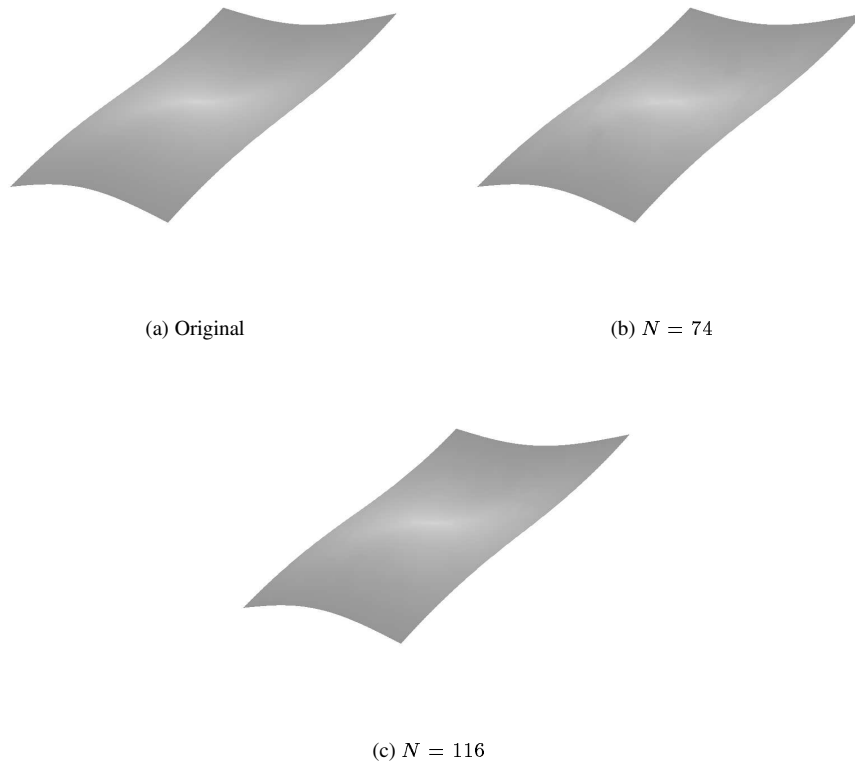


FIG. 5.4. Test function  $f_3$ .

Table 5.1 presents the error of approximation produced by the compression algorithm for various numbers of coefficients. Note that for test function  $f_5$  we have shown less data than for the other test functions. This is due to the fact that the error with respect to  $f_5$  only starts to increase when we have less than 1000 coefficients. This is because the cusp singularity cannot be approximated up to arbitrary precision by the  $C^1$  splines. Table 5.2 compares the theoretical error rates (5.16) to the experimental error rates and shows how much is gained with respect to linear approximation. Figures 5.2 up to 5.6 depict the original test functions together with some compressed approximants. Notice the artefacts in Figure 5.5 (b) and (c). Because the bisector of the unit square  $[0, 1]^2$  is an edge of the initial triangulation  $\Delta_0$ , our compression algorithm needs a lot of derivative information on this bisector (which coincides with the ridge). Therefore, at one side of the ridge, we get a very good approximation because the derivatives are estimated well, and on the other side we get the artefacts.

Finally let us make a comparison with other similar methods in the literature. Since the construction of multivariate wavelets on arbitrary triangulations is very challenging, and, except for box spline spaces, little is known yet about higher order spline spaces, we will restrict ourselves to a comparison with the results of [13]. Here  $C^2$  continuous box splines on uniform partitions are used. As can be deduced from (5.16), the best rate that we can get with the compression method presented here is  $\mathcal{O}(N^{-3/2})$ . This is due to the fact that  $s < 3$  in (5.16) which is a direct consequence of the  $C^1$  continuity of the splines that we use. In comparison, the best compression rate that can be achieved with the  $C^2$  box splines

TABLE 5.1

*Errors and number of coefficients for the surface compression algorithm applied to the test functions  $f_1$ ,  $f_2$ ,  $f_3$ ,  $f_4$  and  $f_5$ .*

| Test function | Error                 | Number of coefficients |
|---------------|-----------------------|------------------------|
| $f_1$         | $5.94 \times 10^{-5}$ | 6666                   |
|               | $1.01 \times 10^{-4}$ | 4156                   |
|               | $4.36 \times 10^{-4}$ | 1455                   |
|               | $6.06 \times 10^{-4}$ | 1175                   |
|               | $1.17 \times 10^{-3}$ | 944                    |
|               | $4.71 \times 10^{-3}$ | 340                    |
|               | $6.45 \times 10^{-3}$ | 258                    |
|               | $8.00 \times 10^{-3}$ | 232                    |
|               | $1.17 \times 10^{-2}$ | 181                    |
| $f_2$         | $6.55 \times 10^{-6}$ | 5610                   |
|               | $1.34 \times 10^{-5}$ | 4838                   |
|               | $4.30 \times 10^{-5}$ | 4094                   |
|               | $1.67 \times 10^{-4}$ | 2664                   |
|               | $5.54 \times 10^{-4}$ | 1156                   |
|               | $1.51 \times 10^{-3}$ | 474                    |
|               | $3.36 \times 10^{-3}$ | 272                    |
|               | $6.35 \times 10^{-3}$ | 152                    |
|               | $1.02 \times 10^{-2}$ | 108                    |
| $f_3$         | $1.12 \times 10^{-5}$ | 2174                   |
|               | $5.67 \times 10^{-5}$ | 798                    |
|               | $9.12 \times 10^{-5}$ | 498                    |
|               | $1.83 \times 10^{-4}$ | 336                    |
|               | $4.15 \times 10^{-4}$ | 198                    |
|               | $6.01 \times 10^{-4}$ | 174                    |
|               | $8.97 \times 10^{-4}$ | 148                    |
|               | $1.10 \times 10^{-3}$ | 116                    |
|               | $2.10 \times 10^{-3}$ | 74                     |
| $f_4$         | $1.10 \times 10^{-5}$ | 2232                   |
|               | $4.99 \times 10^{-4}$ | 1949                   |
|               | $7.87 \times 10^{-4}$ | 1691                   |
|               | $2.42 \times 10^{-3}$ | 1477                   |
|               | $4.27 \times 10^{-3}$ | 725                    |
|               | $6.42 \times 10^{-3}$ | 499                    |
|               | $1.19 \times 10^{-2}$ | 246                    |
|               | $2.25 \times 10^{-2}$ | 125                    |
|               | $3.68 \times 10^{-2}$ | 81                     |
| $f_5$         | $4.26 \times 10^{-4}$ | 1006                   |
|               | $5.02 \times 10^{-4}$ | 868                    |
|               | $1.02 \times 10^{-3}$ | 578                    |
|               | $4.45 \times 10^{-3}$ | 216                    |
|               | $1.08 \times 10^{-2}$ | 114                    |
|               | $4.53 \times 10^{-2}$ | 48                     |

TABLE 5.2

*Theoretical and experimental error rates for the test functions  $f_1$ ,  $f_2$ ,  $f_3$ ,  $f_4$  and  $f_5$ .*

|       | Linear approximation    | Theoretical compression rate | Experimental compression rate |
|-------|-------------------------|------------------------------|-------------------------------|
| $f_1$ | $\mathcal{O}(N^{-3/2})$ | $\mathcal{O}(N^{-3/2})$      | $29.8N^{-1.51}$               |
| $f_2$ | $\mathcal{O}(N^{-5/8})$ | $\mathcal{O}(N^{-5/4})$      | $3.68N^{-1.26}$               |
| $f_3$ | $\mathcal{O}(N^{-3/4})$ | $\mathcal{O}(N^{-3/2})$      | $1.19N^{-1.47}$               |
| $f_4$ | $\mathcal{O}(N^{-1/2})$ | $\mathcal{O}(N^{-1})$        | $3.37N^{-1.03}$               |
| $f_5$ | $\mathcal{O}(N^{-1/4})$ | $\mathcal{O}(N^{-3/2})$      | $24.0N^{-1.62}$               |

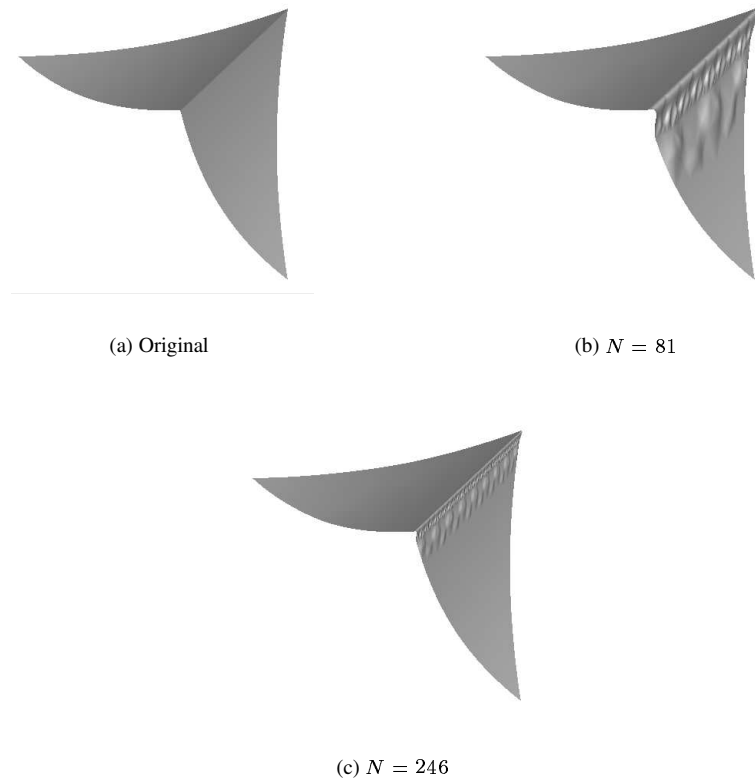


FIG. 5.5. Test function  $f_4$ .

of [13] is  $\mathcal{O}(N^{-2})$ , due to the smoother splines that are used. Table 5.3 shows the error of approximation produced by the compression method from [13] for the test functions  $f_4$  and  $f_5$ . The experimental rates for  $f_4$  and  $f_5$  are given by  $3.36N^{-1.01}$  resp.  $604N^{-2.00}$ . Note that both compression algorithms give almost equal results for test function  $f_4$ . For test function  $f_5$  the compression algorithm of [13] gives an error rate of  $\mathcal{O}(N^{-2})$  which is superior to our error rate, although our method gives better results for  $N$  small.

TABLE 5.3

Errors and number of coefficients for the surface compression algorithm from [13] applied to the test functions  $f_4$  and  $f_5$ . (Results extracted from [13])

| Test function | Error                 | Number of coefficients |
|---------------|-----------------------|------------------------|
| $f_4$         | $1.60 \times 10^{-3}$ | 1934                   |
|               | $6.49 \times 10^{-3}$ | 482                    |
|               | $1.30 \times 10^{-2}$ | 237                    |
|               | $2.59 \times 10^{-2}$ | 116                    |
|               | $4.22 \times 10^{-2}$ | 80                     |
| $f_5$         | $1.38 \times 10^{-3}$ | 618                    |
|               | $2.76 \times 10^{-3}$ | 463                    |
|               | $1.38 \times 10^{-2}$ | 222                    |
|               | $2.69 \times 10^{-2}$ | 163                    |
|               | $7.13 \times 10^{-2}$ | 91                     |
|               | $1.05 \times 10^{-1}$ | 70                     |

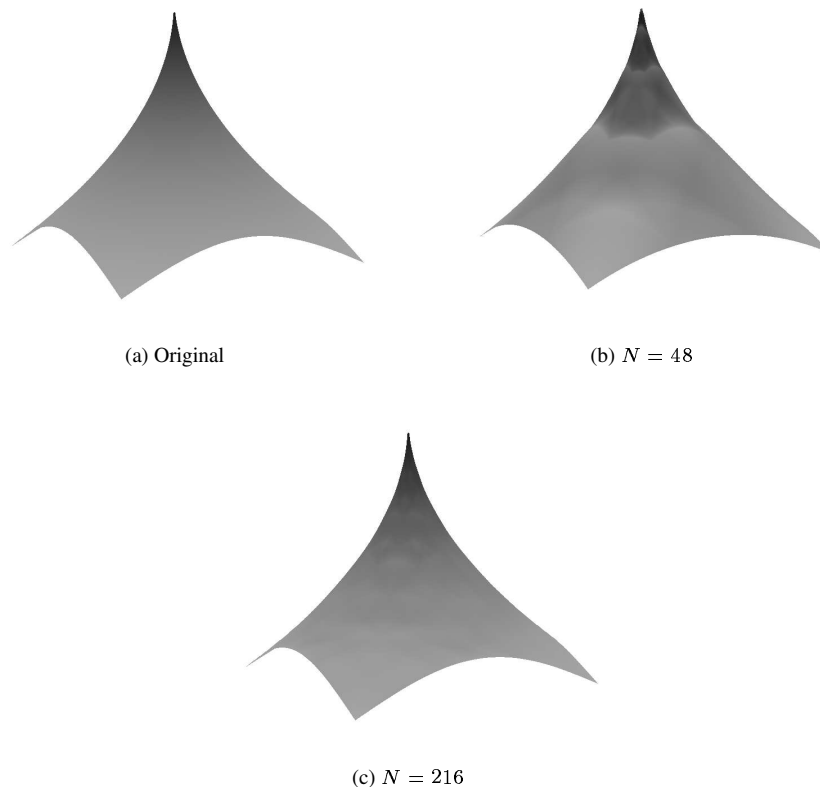


FIG. 5.6. Test function  $f_5$ .

REFERENCES

- [1] R. A. ADAMS, *Sobolev Spaces*, Academic Press, New York, 1975.
- [2] J. H. BRAMBLE AND S. R. HILBERT, *Bounds for a class of linear functionals with applications to Hermite interpolation*, Numer. Math., 16 (1971), pp. 362–369.
- [3] J. M. CARNICER, W. DAHMEN, AND J. M. PEÑA, *Local decomposition of refinable spaces*, Appl. Comput. Harm. Anal., 3 (1996), pp. 127–153.
- [4] C. COATMÉLEC, *Approximation et interpolation des fonctions différentiables de plusieurs variables*, Ann. Sci. Ecole Normale Sup., 83 (1966), pp. 271–341.
- [5] A. COHEN, *Wavelets in numerical analysis*, in Handbook of Numerical Analysis, Vol. VII, P. G. Ciarlet and J. L. Lions, eds., North-Holland, Amsterdam, 2000.
- [6] M. DÆHLEN, T. LYCHE, K. MØRKEN, R. SCHNEIDER, AND H.-P. SEIDEL, *Multiresolution analysis over triangles, based on quadratic Hermite interpolation*, J. Comput. Appl. Math., 119 (2000), pp. 97–114.
- [7] W. DAHMEN, *Some remarks on multiscale transformations, stability and biorthogonality*, in Curves and surfaces, P. J. Laurent, A. L. Méhauté, and L. L. Schumaker, eds., Academic Press, 1994.
- [8] ———, *Stability of multiscale transformations*, J. Fourier Anal. Appl., 4 (1996), pp. 341–362.
- [9] ———, *Wavelet and multiscale methods for operator equations*, in Acta Numerica, Vol. 6, A. Iserles, ed., Cambridge University Press, 1997, pp. 55–228.
- [10] ———, *Multiscale and wavelet methods for operator equations*, in Multiscale problems and methods in numerical simulation, pp. 31–96, C. Canuto, ed., Lecture Notes in Mathematics 1825, Springer Verlag, 2003.
- [11] W. DAHMEN, P. OSWALD, AND X.-Q. SHI,  *$C^1$ -hierarchical bases*, J. Comput. Appl. Math., 51 (1994), pp. 37–56.
- [12] O. DAVYDOV AND R. STEVENSON, *Hierarchical Riesz bases for  $H^s(\Omega)$ ,  $1 < s < 5/2$* , Constr. Approx., 22 (2005), pp. 365–394.

- [13] R. A. DEVORE, B. JAWERTH, AND B. J. LUCIER, *Surface compression*, Comput. Aided Geom. Design, 9 (1992), pp. 219–239.
- [14] R. A. DEVORE AND G. G. LORENTZ, *Constructive Approximation*, Springer-Verlag, Berlin, 1993.
- [15] R. A. DEVORE AND V. A. POPOV, *Interpolation of Besov spaces*, Trans. Amer. Math. Soc., 305 (1988), pp. 397–414.
- [16] R. A. DEVORE AND R. C. SHARPLEY, *Maximal Functions Measuring Smoothness*, vol. 293, Mem. Amer. Math. Soc., 1984.
- [17] ———, *Besov spaces on domains in  $\mathbb{R}^d$* , Trans. Amer. Math. Soc., 335 (1993), pp. 843–864.
- [18] P. DIERCKX, *On calculating normalized Powell–Sabin B-splines*, Comput. Aided Geom. Design, 15 (1997), pp. 61–78.
- [19] G. FARIN, *Triangular Bernstein–Bézier patches*, Comput. Aided Geom. Design, 3 (1986), pp. 83–127.
- [20] G. FARIN, J. H. HOSCHEK, AND M. S. KIM, *Handbook of Computer Aided Geometric Design*, North-Holland, Amsterdam, 2002.
- [21] R. FRANKE, *Scattered data interpolation. test of some methods*, Math. Comp., 38 (1982), pp. 181–200.
- [22] M. J. LAI AND L. L. SCHUMAKER, *On the approximation power of bivariate splines*, Adv. Comput. Math., 9 (1998), pp. 251–279.
- [23] J. MAES AND A. BULTHEEL, *Surface compression with hierarchical Powell–Sabin B-splines*, Int. J. of Wavelets Multiresolut. Inf. Process., 4 (2006), pp. 177–196.
- [24] J. MAES, E. VANRAES, P. DIERCKX, AND A. BULTHEEL, *On the stability of normalized Powell–Sabin B-splines*, J. Comput. Appl. Math., 170 (2004), pp. 181–196.
- [25] C. MANNI AND P. SABLONNIÈRE, *Quadratic spline quasi-interpolants on Powell–Sabin partitions*, 2005, to appear in Adv. Comput. Math..
- [26] P. OSWALD, *Hierarchical conforming finite element methods for the biharmonic equation*, SIAM J. Numer. Anal., 29 (1992), pp. 1610–1625.
- [27] M. J. D. POWELL AND M. A. SABIN, *Piecewise quadratic approximations on triangles*, ACM Trans. on Math. Software, 3 (1977), pp. 316–325.
- [28] P. SABLONNIÈRE, *Error bounds for Hermite interpolation by quadratic splines on an  $\alpha$ -triangulation*, IMA J. Numer. Anal., 7 (1987), pp. 495–508.
- [29] E. A. STOROZHENKO AND P. OSWALD, *Jackon’s theorem in the spaces  $L_p(\mathbb{R}^k)$ ,  $0 < p < 1$* , Siberian Math. J., 19 (1978), pp. 630–639.
- [30] W. SWELDENS, *The lifting scheme: A construction of second generation wavelets*, SIAM J. Math. Anal., 29 (1997), pp. 511–546.
- [31] E. VANRAES, J. MAES, AND A. BULTHEEL, *Powell–Sabin spline wavelets*, Int. J. of Wavelets Multiresolut. Inf. Process., 2 (2004), pp. 23–42.
- [32] E. VANRAES, J. WINDMOLDERS, A. BULTHEEL, AND P. DIERCKX, *Automatic construction of control triangles for subdivided Powell–Sabin splines*, Comput. Aided Geom. Design, 21 (2004), pp. 671–682.
- [33] J. WINDMOLDERS, E. VANRAES, P. DIERCKX, AND A. BULTHEEL, *Uniform Powell–Sabin spline wavelets*, J. Comput. Appl. Math., 154 (2003), pp. 125–142.